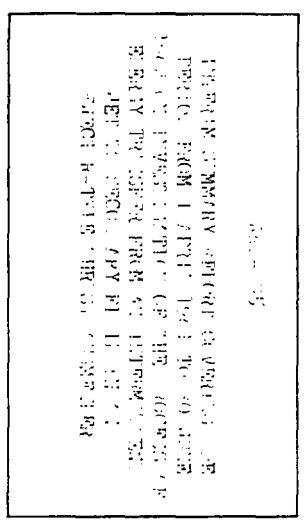

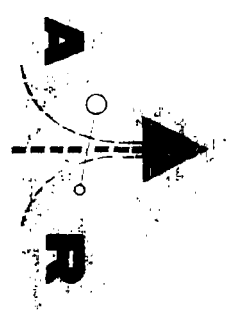

Nonr 3082(00)
R:GAR:mmg
Ser 1333
14 Aug 1963

FIRST ENDORSEMENT on HILLER AIRCRAFT COMPANY ltr ARD63AR8 ERS:hg of 24 Jul 1963

From: Bureau of Naval Weapons Representative, Palo Alto, California
To: Distribution List

Subj: Distribution of Interim Summary Report Covering the Period from 1 April 1961 to 30 June 1962 on Investigation of the Process of Energy Transfer from an Intermittent Jet to Secondary Fluid in an Ejector-Type Thrust Augmenter, Contract Nonr 3082(00), Hiller Report No. ARD-305

1. Forwarded for information and comment, if appropriate.

G. A Robinson
G. "A" ROBINSON

Copy to:
Hiller Aircraft Co.

PALO ALTO, CALIFORNIA • CABLE ADDRESS "HILLER" • TELEPHONE 325 1241

HILLER AIRCRAFT COMPANY

In Reply Please Refer to:
ME63AR8 ERS:hg

July 24, 1963

To: Distribution List

Via: Bureau of Naval Weapons Representative,
Palo Alto, California

Subject: Distribution of Interim Summary Report Covering the Period from 1 April 1961 to 30 June 1962 on Investigation of the Process of Energy Transfer from an Intermittent Jet to Secondary Fluid in an Ejector-Type Thrust Augmenter, Contract Nonr 3082(00), Hiller Report No. ARD-305

Encl.: (1) Subject Report

1. Subject report is hereby transmitted to the addressees listed in the Distribution List per instructions of the Office of Naval Research, Code 461.

2. We would like to hear from you, if this report raises any questions or comments.

HILLER AIRCRAFT COMPANY

E. R. Sargent
Manager, Propulsion Dept.
Advanced Research

Report No. ARD-305

30 June 1962

INTERIM SUMMARY REPORT COVERING THE PERIOD FROM 1 APRIL 1961 to 30 JUNE 1962 ON INVESTIGATION OF THE PROCESS OF ENERGY TRANSFER FROM AN INTERMITTENT JET TO SECONDARY FLUID IN AN EJECTOR-TYPE THRUST AUGMENTER

A Research Program Conducted For
Office of Naval Research, Air Programs
Department of the Navy
Contract Nonr 3082(00)

Raymond M. Lockwood
Principal Investigator

W. G. Patterson
Research Engineer

ADVANCED RESEARCH
DIVISION OF HILLER AIRCRAFT COMPANY

FOREWORD

This report covers the third phase of the Investigation of the Process of Energy Transfer from an Intermittent Jet to Secondary Fluid in an Ejector-Type Augmenter under Office of Naval Research Contract Nonr 3082(00). The first and second phases are covered in References 2 and 3.

The principal investigator wishes to acknowledge the assistance from his associates at Hiller:

D. A. Graber for set-up and operation of test equipment and assistance in conducting the experiments;

W. G. Patterson for conducting the experiments and for providing analysis and evaluation of test procedures and equipment;

H. W. Sander for assistance in data analysis and report preparation.

Appreciation is expressed for the generous expenditure of time in a discussion of the problem of analysis and for encouragement by Dr. Joseph V. Foa, Professor of Aeronautical Engineering at Rensselaer Polytechnic Institute.

Acknowledgment is made of the important assistance in the application of the Vector-Polar Method of analysis of wave interactions by the following people of the University of California Detonation Laboratory who acted as consultants:

Dr. A. K. Oppenheim, Professor of Aeronautical Engineering at the University of California, Berkeley, author of over 70 technical publications on the subjects of fluid mechanics, dynamics and combustion;

Dr. Arnold Laderman, Research Engineer at the University of California Detonation Lab;

Mr. Paul Urtiew, Graduate Research Engineer at the University of California.

Although the advice and assistance received from others have contributed greatly to the progress of the investigation, the final responsibility for the direction and results of the project rests with the Principal Investigator.

SUMMARY

Previous reports on this project have emphasized the unusually high thrust augmentation possible with relatively small ejector-type thrust augmenters when the jet is intermittent instead of steady. It has been postulated that the high performance is achieved by the process of pressure wave energy transfer and does not depend on mixing of the primary and secondary fluid. The current phase of the investigation has shown correlation between analysis and test data. Improved experimental techniques were used, including color schlieren streak photography and high speed pressure transducer records.

Two analyses have been made, each being a graphical-numerical solution to the non-linear partial differential equations of unsteady one-dimensional gas dynamics. The first is the detailed "in the small" use of wave diagrams in the physical (x-t) plane in conjunction with the classical numerical method of calculations called "Method of Characteristics". The second is the newer "Vector-Polar Method" which deals with wave and fluid velocity interactions only "in the large". The latter is based on a combination of two plots, (a) the (x-t) physical plane and (b) the vector plot of the natural logarithm of pressure ratios across each major compression fan, shock wave, and rarefaction fan versus the change of particle velocity ratio.

The device for converting steady flow to intermittent jets has been used in conjunction with color schlieren and high-speed pressure instrumentation and is shown to be an excellent research tool for creating intermittent jets with a range of velocities and wave forms not possible heretofore. This device also appears to have potential as a high-performance thrust augmenter for turbojet lift engines.

TABLE OF CONTENTS

FIGURE LIST

FIGURE LIST (CON'T)

INDEX OF SYMBOLS

1. INTRODUCTION

The period covered by this report constitutes the third phase of the investigation of the energy transfer process from an intermittent jet to a secondary fluid in an ejector type thrust augmenter under Contract Nonr 3082(00). The second phase is covered in Hiller Aircraft Corp. report ARD-286 (Ref. 3) while the preliminary investigation or first phase is covered in ARD-238 (Ref. 2).

In the final report of the first phase work (ARD-238), the mechanism of thrust augmentation of intermittent jets was postulated on the idea that the intermittent jet acts as a piston as it enters and travels through the augmenter. Verification of this idea through flow visualization led to the conclusion that for analysis, the assumption of no mixing between the primary jet and the secondary fluid would be appropriate. The main exchange of energy takes place as a direct exchange of pressure between the jet piston and the secondary fluid. Comparison with a steady flow ejector, in which the energy exchange between the primary jet and secondary fluid occurs through a mixing process, emphasizes the novel characteristics and superior performance of the intermittent jet thrust augmenter. For example, an augmenter with a throat area-to-primary jet area ratio of 4 and a length-to-throat diameter ratio of 1-1/2, when used with an intermittent jet, can produce a thrust equal to anywhere between 60% to 140% of the primary jet thrust depending on the augmenter configuration and the intermittent jet wave form and velocity. The same augmenter and primary jet relationship for the case of steady flow would produce less than 20% thrust augmentation.

The second phase of the investigation (ARD-286) produced a more refined description of the intermittent jet energy exchange process. The approach was that of developing improved flow visualization and investigating various augmenter geometries and their effect on fluid flow rates, thrust and primary jet performance. Concurrently, a search for methods of analysis was accomplished. In addition, various types of devices were considered for production of intermittent jets. Several piston-in-tube

mechanisms were designed and tested, as well as a mechanical valve for converting a steady flow to an intermittent flow without creating disturbances upstream. Most extensive use to date, however, has been made of the small valved pulsejets, such as the Dynajet and Tigerjet, and the valveless pulsejet-augmenter combination called the Pulse Reactor which is being developed by Hiller as a lift-propulsion device (Refs. 10 and 11). It is with this valveless combustor that 140% thrust augmentation was achieved using an augmenter configuration developed during this phase of the program. As a result of this development, the Pulse Reactor has achieved performance which is competitive with that of turbojet engines as far as static performance is concerned (i.e., thrust specific fuel consumption of better than 1 pph/lb. Additional characteristics of the Pulse Reactor which make it attractive as a lift-propulsion device are a thrust-to-weight ratio of 10:1, low downwash temperatures and velocities of approximately 200°F and 200 ft/sec, refusal to ingest foreign particles, simplicity, low cost and many others. Further development through study of the intermittent jet thrust augmenter will, undoubtedly, contribute additional gains to its performance.

In the third phase of the energy transfer investigation, covered by this report, we have sought to develop the theoretical analysis and to provide some data for its support. Piezoelectric pressure transducers were installed in the augmenter walls in order to measure the magnitude of the pressures created by the motion of the jet piston through the augmenter. After much careful attention to the details of installation and to the spurious response of the transducers, such as thermal drift and vibration sensitivity, satisfactory pressure measurements were made. These were synchronized time-wise with the high speed schlieren motion pictures and schlieren streak photography. Improvements in the schlieren photographic technique have resulted in the observation of the pressure waves and their reflections from the end of the augmenter.

Analysis of the intermittent jet augmenter is being pursued on the basis of one-dimensional unsteady gas dynamics. The basic equations

are non-linear partial differential equations which in general are not amenable to direct solution. However, there are two useful numerical-graphical methods of solution which are recommended. The first is the classical Method of Characteristics utilizing time-distance wave diagrams. This is a method of detailed analysis "in the small" as contrasted to the Vector-Polar Method which is an analysis "in the large". The latter method is a new and powerful analytical tool for study of wave interactions that ignores the detailed interactions at a considerable saving of computations in many cases.

Several tests of the converter device for producing an intermittent jet from a steady flow were conducted. Schlieren photographs revealed the pressure waves and reflections more clearly than in the case of the small combustion-driven pulsejets. The lower temperatures of the jet pulse also contributed to less thermal drift effect of the pressure transducer signals. Various jet wave forms and velocities may be produced with this device to broaden the experimental observations of the augmentation phenomena. These factors appear to make the converter a desirable tool for further work in this investigation. Of greater significance, however, is the performance of the converter in terms of thrust and augmentation ratio. While the initial tests did not show anything on the order of phenomenal results, they did show that the steady flow may be converted efficiently into a pulsing jet and, with a potential augmentation ratio of 2.0 or higher, produce a sizeable gain in thrust over the steady flow case. Not only thrust, but pumping rates of ejectors against various pressure heads can be improved through this approach.

The importance of this investigation into pulsating flow is apparent from the magnitude of the performance indicated. In fact, interest in general in pulsating and unsteady phenomena is rapidly increasing due to higher performance demands from "steady flow" equipment and the problems this creates in engineering, as well as to the promising performance of systems specifically designed for unsteady flow conditions. Development of the shock tube over the past several years has contributed greatly to methods of analysis of waves and transient gas dynamics. Recent developments in

instrumentation and visualization techniques have added new momentum to research and development in unsteady flow fields. The results can be described as significant and rewarding.

2. EXPERIMENTAL RESEARCH

2.1 Flow Visualization

The Fairchild HS-101 high speed motion picture camera and color-modified schlieren photographic system have provided excellent visualization of the intermittent jet and ambient fluid flow through the augmenter. This equipment is described in ARD-286 (Reference 3). Experimentation with various light sources has led to the conclusion that a tungsten filament G.E. No. 1927 12-volt bulb operated at 18 volts is satisfactory in most aspects for motion picture color and black-and-white photography. Ektachrome ER type B, and Tri-X reversal film are used.

A multicolored filter, which is made of adjacent bands of gelatin filter material of contrasting colors, is used in place of the conventional schlieren knife-edge for color photography. The image of the tungsten filament light source is then focused on a particular band of color giving a uniform background color on the film plane. By using an asymmetrical filter array with respect to the background color, the direction of the density gradient in the flow under observation may be determined. For example, a filter with a green background color with red to the left and blue to the right will show compressions as blue and rarefactions as red in our particular set-up. By using the color filter array, all the schlieren light passes through to the viewing plane. The color shown in the photograph at each point in the field is then proportional to the density gradient in the direction normal to the edges of each color strip in the filter. Geometry of the double pass Hiller schlieren system is shown in figure A which illustrates the change of color depending upon the degree of refraction by the density gradient. The reader will note that in the presence of a density gradient the image appears in the same position as if there were no gradient but is illuminated in a different color.

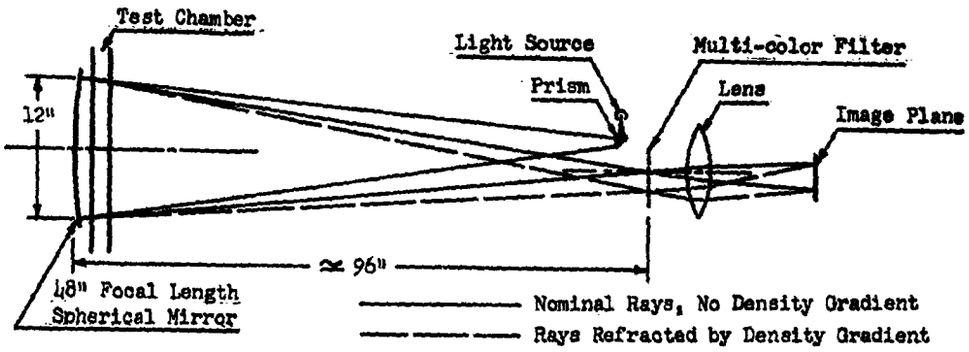

FIGURE A: SCHEMATIC OF HILLER DOUBLE-PASS COLOR SCHLIEREN SYSTEM

In order to understand the effect of densities on the schlieren light rays, the following analysis is made. First, the refractive index is the ratio of the velocity of light in a vacuum to the velocity of light in the substance. This ratio is a function of the wavelength of the light, but since the total refraction studied in most cases is small and since the wave-length dispersion is much smaller, the dispersion effect is not considered. The use of monochromatic light, of course, would eliminate the dispersion effect.

The following symbols are used:

c_o = velocity of light in a vacuum
t = time
c = velocity of light in a medium
n = index of refraction = c_o/c
ρ = gas density
K = Gladstone-Dale constant
r = specific refraction
α = angle of refraction
R = distance normal to light ray
S = path of a light ray

ΔS = distance wave front travels along light ray b

γ = angle between refractive index gradient and light ray

$\vec{e}$ = unit vector indicating the direction normal to the light ray

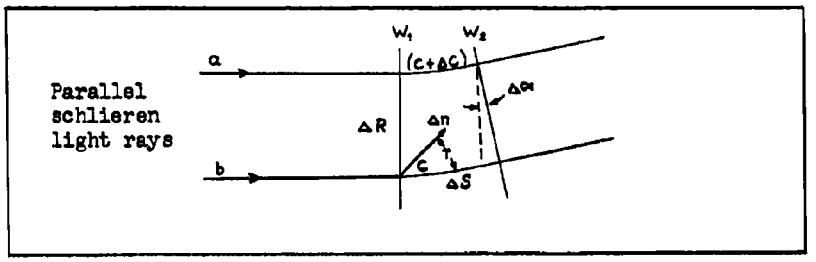

FIGURE B

In Figure B, W_1 is a wave front, W_2 is the same front at Δt later, and a and b are light rays orthogonal to the fronts. The ray or wave front is turned through the angle ($\Delta\alpha$) by the refractive index gradient at an angle γ to the ray. Then:

$$(\Delta S = c\Delta t) \qquad (1)$$

$$(\Delta\alpha = \frac{-\Delta c\ \Delta t}{\Delta R}) \qquad (2)$$

where Δc is the difference in velocity of W_1 and W_2 between the two light rays a and b.

Combining equations (1) and (2):

$$\Delta\alpha = -\frac{\Delta c}{c}\frac{\Delta S}{\Delta R} \qquad (3)$$

then as ΔS and ΔR o:

$$d\alpha = -\frac{dc}{c}\frac{dS}{dR} \qquad (4)$$

also $n = c_o/c$ or $\frac{dn}{n} = -\frac{dc}{c}$

then: $d\alpha = -\frac{n}{R}\frac{dS}{n}$

or $d\alpha = \frac{1}{n}(\vec{e}\cdot \text{grad } n)dS$ (5)

where $\vec{e}$. grad(n) is the component of the vector gradient of the n field in the $\vec{e}$ direction.

The Lorens-Lorentz equation gives the relation between the refractive index and the density.

$$r\rho = \frac{(n+1)(n-1)}{(n^2+2)} \qquad (6)$$

where r is called the specific refraction and is nearly a constant for each medium.

In the case of a gas, since n is very close to 1,

$\left(\frac{n+1}{n^2+2}\right)$ also may be considered a constant in comparison to (n-1).

Then, $$n = 1+K\rho \qquad (7)$$

where K is the Gladstone-Dale constant or:

$$n = 1+\beta\ \rho/\rho_s$$

where ρ_s, the reference density, is taken at standard conditions and β is a dimensionless constant. Values for n, ρ_s and K are given in Table I.

Differentiation of equation (7) gives:

$$\frac{dn}{d\rho} = K = \beta/\rho_s \qquad (8)$$

Combining with equation (5):

$$d\alpha = K(\vec{e}.\text{grad}\ \rho)dS \qquad (9)$$

Referring to Figure C in which a refractive index (or density) gradient and the test section thickness ℓ are small compared to K, thus leading to small angles of deflection, α may be approximated by

$$\alpha = K\int_0^{\ell} \frac{\partial\rho}{\partial x}\,dy \qquad (10)$$

where $\frac{\partial \rho}{\partial x}$ is the local density gradient normal to the schlieren light rays. Furthermore, if the flow is one-dimensional so that conditions are the same for every x-plane, the integral gives

$$\alpha = K\ell \frac{\partial \rho}{\partial y} \qquad (11)$$

TABLE I

n and ρ_s at 32°F, 14.7 psia

$\lambda = \lambda_D = 5893A$

Gas	n	ρ_s lb/ft^3	K ft^3/lb
Air	1.000292	.08071	.003618
Nitrogen	1.000297	.07807	.003804
Oxygen	1.000271	.08921	.003038
Carbon Dioxide	1.000451	.1234	.003655
Water Vapor	1.000254	.05026	.005054

Our particular set-up is a single mirror system which passes the schlieren light twice through the flow field. With the assumption that each light ray, when reflected from the mirror, passes very close to its first path, the total deflection angle is then equal to 2α.

For a constant pressure process, equation (10) combined with the perfect gas law yields:

$$\alpha = -K \frac{P}{R} \int_0^{\ell} \frac{1}{T^2} \frac{\partial T}{\partial x} dy \qquad (12)$$

where P, T, and R are the pressure, temperature and gas constant.

For the isentropic process,

$$\alpha = \frac{K}{kRT_o} \int_o^{\ell} \left(\frac{P_o}{P}\right)^{\frac{k-1}{k}} \frac{\partial P}{\partial x}\, dy \qquad (13)$$

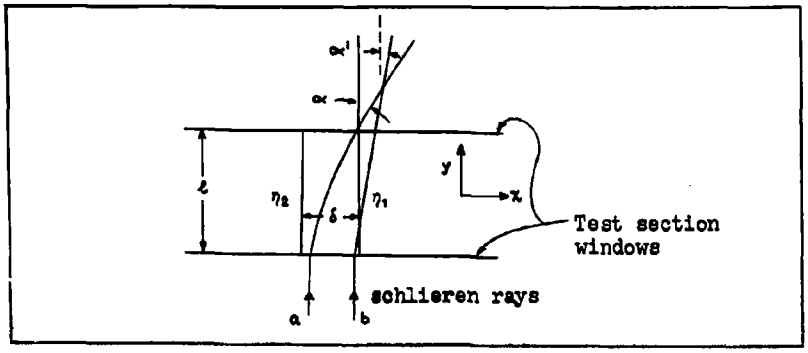

FIGURE C

where k is the ratio of specific heats.

Large density gradients which occur in a very short distance, such as shock waves and interfaces, require a different analysis. In such cases a schlieren light ray may be deflected out of the gradient region. In Figure C a large refractive index gradient, such as a plane shock wave, of thickness δ separates regions with refractive indexes of n_1 and n_2. The ray which remains in the zone the longest is the one which is deflected through the largest angle. For simplicity, it is assumed that the refractive index gradient is uniform across δ. Then from equation (5)

$$\alpha = \frac{\Delta n}{\delta} \frac{y}{n} \qquad (14)$$

where α is the change in direction of the deflected ray and y is the distance through which the ray remains inside the gradient region. The different deflections and resulting displacements of rays entering the same density gradient region causes a superposition of 2 or more colors in the film plane when the multicolor filter is used, and a reduction in contrast resolution in the case of the knife-edge schlieren.

The Hiller schlieren system consists of a single 12" spherical mirror

of 48" focal length arranged so that the central axis of the light source is close to the camera axis. This permits the light beam to pass twice through the schlieren field to provide double sensitivity. The mirror and schlieren head are mounted on drill press stands so that alignment adjustments can be easily made. Other advantages of such a system are its low cost, due to minimum number of elements, compactness (96" from mirror to knife edge), simplicity and portability. There are, however, several deficiencies in the system. Because the light source axis cannot be made to coincide with the camera axis, there is some coma present. The two light paths through the field are not coincident due to the refraction in the field, as well as to the off-axis light source, which impairs the resolution of the image. Furthermore, since the light rays are divergent-convergent and the field of study is plane, a curvature of field aberration is present.

Reference (3), Hiller ARD-286, presented examples of the color schlieren photography by means of 35 mm projection slides composed of selected frames and streaks from the motion pictures. In addition, Air Branch, Office of Naval Research, has been furnished film sequences representing the color schlieren and black-and-white photography.

Figure 1 illustrates the results of the schlieren flow visualization studies. A pressure wave caused by combustion and motion of the gases in the tailpipe of the jet engine is not shown in the sketches. This wave is frequently visible emerging from the pulsejet tailpipe slightly ahead of the jet. In the case of the mechanically produced intermittent jet (converter described in section 2.4) operated at optimum thrust (tuned to resonance) this wave is clearly visible in the motion pictures. The streak pictures provide information from which the pressure wave velocities and particle velocities are determined.

From the motion picture studies the augmentation action may be described qualitatively as follows: The jet pulse enters the augmenter and forms a seal with the augmenter walls. As it travels through the augmenter, its energy is transfered to the fluid in front of it by means of the pressure waves which are visible in the schlieren streak photographs. The

ambient air is thus pushed out of the augmenter. The jet pulse then separates from the jet tailpipe and continues through the augmenter. Ambient air is drawn in behind the pulse, again, by a pressure wave energy exchange process. In this way the augmenter is filled with ambient air ready to begin a new cycle.

2.2 Instantaneous Pressure Measurements

Instantaneous pressure measurements along the augmenter wall still continue to present problems. However, we have fairly well identified these problems and considerable progress has been made in their solution. The earliest pressure measurements in our program were made with the use of a Consolidated Electrodynamics Corp. type 4-316A (± 7.5 psig) strain gage transducer with a sensitivity of ± 10 mv full range. Because of its relatively low frequency response (approximately 7000 CPS) and low damping, it was not suitable for our application as is later demonstrated by comparison of oscilloscope pressure trace recordings (Fig. 7). Currently in use are Kistler miniature piezoelectric quartz pressure transducers (model 601) coupled with the Kistler Model 566 charge amplifiers. This system is excellent from the standpoint of fast response. However, there are certain disadvantages which are magnified in our particular application. The pressures we are measuring are in the order of ± 5 psig. In this pressure range, the resolution of the transducer is adequate, but the output is so small that a great deal of amplification is necessary (at least 1 picocoulomb/cm overall). As a result, great care must be taken in the test set-up and associated amplifiers in order to minimize the noise-to-signal ratio.

Figure 2 shows the majority of the electronic equipment used in association with the piezoelectric pressure transducers. This equipment consists of a dual-beam oscilloscope with a Polaroid camera, two miniature charge amplifiers, a pre-amp with two chopper switches and a simultaneous electronic switch for connecting five circuits at a given signal. The choppers allow up to four signals to be displayed on the oscilloscope as shown in Figure 3.

2.2.1 Transducer Signal Noise

Some of the sources of transducer signal noise which were discovered include RF signals from nearby radio transmitters, the pulsejet ignition system, microphonics in the electronic equipment, vibration-acceleration response of the transducer, thermal drift of the transducer,

charge leakage, and ground-loops. The first problem approached was that of microphonics in the electronic equipment. Figure 4 shows the magnitude of this signal. This trace was produced by the high acoustical noise level created by the pulsejet while the transducers were disconnected from the charge amplifiers. The solution of this problem was accomplished by installing all of the electronic equipment in an acoustically insulated room, or quiet room, as shown in Figure 2. The ground-loop problem is also apparent in Figure 4 as a 60 cycle ripple in the zero psig reference trace. This problem can be rather mysterious sometimes, but careful attention to the connections and grounds throughout the system is, in most cases, effective. Similarly, RF and ignition noise can be minimized by insuring that all connections, cables, etc., are shielded properly.

Another problem which required considerably more attention was that of the acceleration or vibration response of the quartz transducer. Figure 5 illustrates this problem. The top trace is from a transducer mounted rigidly in the augmenter wall with the transducer face flush with the inner surface of the wall. The lower trace is from a transducer mounted in a blind hole in the augmenter wall. One might say that within the pressure range being measured, the piezoelectric transducer makes a better accelerometer than a pressure transducer. Figure 6 illustrates the mechanical ringing of the augmenter assembly and its effect through acceleration response of the Kistler transducers. In this case both transducers were mounted in the augmenter wall with rubber "O" ring seals. The disturbance was created by tapping the augmenter assembly with a screwdriver.

The pulsejet is a source of strong vibrations, especially if there is a rigid connection between the engine and the augmenter assembly in which the transducers are mounted. The pressure fluctuations on the augmenter walls, however, constitute the greatest part of the vibration problem. By installing the transducer itself in a high density, large mass adapter and then mounting the adapter in the augmenter wall with soft "O" ring seals or equivalent, a substantial reduction in the acceleration noise is achieved.

In order to test various mounting techniques, a small vibrator was constructed consisting of a variable speed motor with a spur gear on its shaft which rubbed against a small hinged beam. An augmenter wall section was clamped to the beam and several transducer mounting schemes were tested. By varying the motor speed, the natural frequency of the mounts could be determined and a comparison of their response made. Several types of mounts which satisfactorily minimized vibration response are sketched in Figure D. A thin layer of silicone grease mixed with asbestos fiber is smeared over the face of the transducer and into the small gap between the adapter and the augmenter wall. This helps shield the transducer face from thermal effects and provides a smooth augmenter wall surface as well as helping the pressure seal.

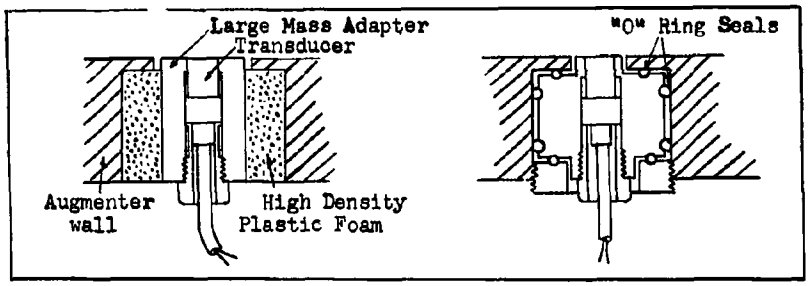

FIGURE D

Acceleration transients or even pressure transients, if they are sufficiently rapid, can excite the transducer at its resonant frequency. Figure 7 shows a comparison of the Kistler and C.E.C. transducer response during pulsejet operation. It is apparent that the C.E.C. transducer is being excited at its resonant frequency (approximately 7000 cps) while the Kistler is not. The natural frequency of the Kistler transducer was later determined to be approximately 125,000 cps.

The most perplexing problem, however, has been the thermal response of the transducer combined with charge leakage, which produces an unstable zero psig reference level. It is desirable to operate the pressure instrumentation with DC coupling to the scope in order to record

the average pressures as well as the pressure transients inside the augmenter. The technique for photographing pressure traces is to first establish a zero psig trace and then after a few seconds of pulsejet operation double expose or superimpose the pressure trace on this signal. The piezoelectric system's sensitivity to thermal effects and charge leakage have not allowed us to establish a creditable zero psig reference. For instance, Figure 8 is a comparison of the pressure traces from a Kistler and a C.E.C. strain gage type transducer. The upper trace is from the piezoelectric transducer with an over-all amplification equivalent to approximately five psig per centimeter. The lower trace is from a C.E.C. transducer with a vertical amplification of about 7.5 psig per centimeter. The oscilloscope sweep speed is 1/2 second per centimeter and the signals are DC coupled to the scope. A brief burst of pulsejet operation has the affect shown in the figure.

A water-cooled adapter was installed with one of the Kistler transducers in an attempt to control the thermal drift. Figure 9 is a comparison between the uncooled transducer and the water-cooled transducer. Both transducers are DC coupled to the scope. The thermal drift was induced by directing a hot air stream (about 250°F) from a small hair dryer on the transducers. The vertical sensitivity is approximately 2 psi per centimeter for both traces. It is obvious that the water-cooled transducer whose signal is displayed on the lower trace has much less thermal drift than the uncooled transducer. The Oscilloscope sweep speed for this photograph was 1 second per centimeter.

Although we have made considerable progress in isolating and in identifying the problems with the pressure transducer systems, we still have not fully resolved the thermal sensitivity and charge leakage problem. As a result, we can expect good transient response from our system, but the static or DC response mode of operation, which is so necessary for referring our pressure traces to the atmospheric condition, has not been reliable. We are considering the possibility of, and errors associated in, combing the A/C coupled transient response displayed on the oscilloscope with the average static pressure measurements, as measured by a manometer, at the

same location as the transducer in the augmenter wall. Finally, in Figure 10, a comparison can be made between a clean trace and a noisy trace. The lower trace illustrates the success of our efforts in resolving these instrumentation problems. However, it should be remembered that the zero psig reference line is not reliable.

2.2.2 Transducer Calibration

The piezoelectric transducer system, according to the manufacturer, can be statically calibrated using a dead-weight gage tester. However, we did not choose to use this method because of the noticeable drift and charge leakage as observed in the pressure signals. Dynamic calibration can be accomplished with the use of a shock tube, or even more simply, with the set-up sketched in Figure 11. This consists of a tank with a three-way solenoid operated valve between its outlet and a pressure chamber in which the transducer is mounted. The transducer is exposed to the atmosphere until the solenoid is actuated which then exposes the transducer to the pressure in the tank. The step function is rapid, especially if the pressure chamber is small. The pressure in the tank is observed on a manometer and changes very little during the calibration procedure. Figure 12 shows the type of output signal observed on the oscilloscope.

The sensitivity of the transducer as determined by this calibration procedure, was calculated to be 0.45 pcb/psi, while the sensitivity as stated by the manufacturer is 0.48 pcb/psi. The difference can possibly be accounted for in amplifier response or calibration, or in the differences in calibrating procedure.

Figure 12 also presents an example of charge leakage or signal drift that is characteristic of the system. The oscilloscope sweep is triggered by the switch which activates the solenoid valve. The slight delay in the solenoid operation is sufficient for a small portion of the trace to record the atmospheric pressure. As the valve opens, the pressure rises and the vibration of the valve against its stop is also recorded in the trace. The solenoid switch is then opened, again exposing the transducer

to atmosphere. The drop in pressure is also recorded in the photograph. The procedure takes less than 1/2 second, however, even though the input is DC coupled to the scope, the charge leakage is apparent as approximately 1/2 centimeter difference in the atmospheric reference portion of each trace.

2.2.3 Oscilloscope Trace Photography

A Tektronix type C-12 oscilloscope camera with a Polaroid roll film camera back is used for the oscilloscope photography. Polaroid 200 speed (Type 42) and the 3000 speed (Type 47) film have been used successfully; however, the 2000 speed film has proven to be the best for a wide range of photography.

The majority of our photography has been of single sweep traces. To insure that no more than one trace is recorded at a time, the scope is equipped with an end-of-sweep lockout. After a short interval of experimentation with the camera, very satisfactory photographs were consistently produced. A simple and successful procedure is as follows:

a. After the scope vertical amplification, trace position, sweep speed, etc. are adjusted to the desired values, the grid illumination is turned off and the sweep trigger control set to the external position. In our set-up, a photoelectric cell provides the signal to trigger the sweep.

b. The camera f stop and the beam intensity are adjusted to values predetermined by experiment. Sufficient time must be allowed for the persistence in the CRT phosphor to die away; then, the sweep control is armed, the shutter opened and the oscilloscope and camera are ready for operation.

c. After the sweep has been recorded, the grid can be photographed by a double exposure.

Occasionally, the oscilloscope beam will not have sufficient intensity for all parts of the trace to be recorded on the photograph. In such a case the trace is usually visible on the "negative" or direct exposure part of the film.

2.3 Fluid Temperature Measurements

Further consideration of the ultrasonic thermometer technique has led to the conclusion that it would be of little value in our application. The technique consists of the observation of small pressure disturbances with the schlieren system. A piezoelectric crystal driven at high frequencies by an oscillator is the source of disturbances. From the frequency and the observed wave length, the speed of sound and thus the temperature may be calculated. The equipment has been described more fully in ARD-286 (Ref. 3).

The drawbacks of this technique are concerned with the method of observation and the nature of the fluid flow. First, the schlieren system must be extremely sensitive in order to make the extremely small disturbance density gradients visible. Due to the large density gradients in the intermittent jet flow situation, especially when the pulsating jet is hot with respect to the ambient fluid, the sensitivity of the schlieren system has been intentionally reduced for best visualization. The conflicting requirements for high sensitivity to observe the small disturbance density gradients and low sensitivity to observe the large density gradients cannot be achieved with the knife-edge system and can only be partially achieved with the color system.

For example, consider a very small density gradient superimposed on a much larger density gradient as would be the case of acoustic disturbances in a region of large thermal gradients. In terms of schlieren light ray deflection, this would be small deflections superimposed on much larger deflections. For observation of these deflections, they must cause a noticeable increase in intensity of light on the film, and in the case of color schlieren, an additional noticeable difference in color. If the background intensity at a point or in a small region, is created by schlieren rays which completely pass the knife-edge, or which are completely blocked by the knife-edge, then it is quite probable that additional small gradients will not change this intensity. Also, the ability to distinguish a change in intensity

is limited by the resolution and sensitivity of the film and eye, and depends strongly on the background intensity and color as well as the size of the disturbance region. It should be expected then that there would be difficulty in distinguishing small acoustinc disturbances in a field of large density gradients. In the case of the color schlieren system, the range of schlieren ray deflections (gradient magnitudes) which can be distinguished is increased by the greater range of contrast afforded by the various colors in the filter, but the small changes must still be within the resolving powers of the film and eye.

Another factor in consideration is the direction of the gradient to be observed. The gradients observed are only those which have components that are perpendicular to the knife-edge. Considering a one-dimensional flow situation in which the fluid properties are functions of the one coordinate in the direction of flow, the knife-edge should be perpendicular to the direction of flow. Then, in order for the acoustic disturbances from the ultrasonic thermometer to be visible, they must also travel in the direction of flow and the fluid velocity must be taken into consideration in calculating the speed of sound. If the acoustic disturbances are introduced perpendicular to the flow, the flow velocity may be omitted from the calculation. Schlieren visualization must then be achieved with the knife-edge at 45° to the flow direction. If the flow, in actuality, is not strictly one-dimensional (as in our application), unknown flow velocity components in the direction of the acoustic propagation introduce errors in the temperature calculation. The thermal gradients and turbulence in the hot intermittent jet piston excessively complicate the ultrasonic thermometer techniques.

Several alternate methods of temperature measurements are being considered. A NANMAC thermocouple is being investigated as a temperature transducer. The elements consist of 2 thin ribbons of thermocouple material insulated from each other by thin ribbons of mica. The junction consists of many microscopic burrs created by rubbing the tip with a piece of emery cloth. It is characterized by very fast response (order of 10

micro seconds), but is limited to temperature measurements at surfaces such as the augmenter wall.

2.4 Intermittent Jet Devices

Many devices can be envisioned for producing intermittent jets. Combustion-driven valveless and valved pulsejets, piston-in-tube mechanisms, and converters for changing steady flow into intermittent flow have all been investigated to some degree. Another interesting concept is the resonant boiler in which water is flashed into steam to provide the driving pressure for each jet pulse. Each of these, of course, has its characteristics and advantages in specific applications.

2.4.1 Valved and Valveless Pulsejets

Most of the testing throughout the program has been done with small valved pulsejets. The commercially available Dynajet and a smaller Japanese copy called the Tigerjet were used. These engines provided an economical and trouble-free primary jet source. In addition, they have been the subject of numerous investigations and much knowledge about their operation and characteristics is on record.

The valveless pulsejet provides a basically simpler mechanism than the valved pulsejet for producing intermittent jets and has shown a higher performance potential in development tests. However, miniaturization, or scaling down, of the valveless pulsejet to a size compatible with the flow visualization and test equipment introduces starting and fuel feed problems which make it less advantageous than the valved pulsejets. The full scale valveless pulsejet with thrust augmenters has been undergoing development here at Hiller Aircraft Company as an aircraft vertical lift-propulsion engine, (Refs. 10 and 11). This combination, called the Pulse Reactor, has demonstrated unique advantages in such applications where susceptibility to foreign object damage, downwash velocities and temperatures, as well as initial cost and complexity, must all be minimized. This type

of propulsion system points out the practicability of a mechanism that is specifically designed for an unsteady flow mode of operation.

2.4.2 Piston-in-Tube Devices

A mechanically driven piston-in-tube device, for operation in water, was designed, built and tested under the previous program (Ref. 3). The cyclic rate of this device was, however, limited to about 10 cycles/sec due to cavitation. Although the performance as a thrust device did not seem to be promising, its use as an analytical tool was satisfactory.

2.4.3 Converter from Steady Flow to Intermittent Flow

Initial tests of the converter (described in ARD-286, Ref. 3) at very low supply pressures have shown intermittent jet thrust augmentation ratios as high as 2.5. With this device there is the possibility of efficiently converting a steady flow to an intermittent flow and taking advantage of the high intermittent jet thrust augmentation ratios to produce a high overall augmentation ratio. In addition, the device allows the "tailoring" of a wide variety of intermittent jet pulse configurations by variations in the valve and port relationships. Blow-down-to-refill time ratio of the intermittent jet tube is quite important from the standpoint of augmentation capability and is well worth investigating. This device can be operated at higher pressure ratios and is comparatively cooler than the pulsejet primary intermittent jet. From this standpoint, it will be a valuable tool for further investigation of the energy transfer process.

Figure 13 is a photograph of the converter and test set-up. Scales measure the augmenter thrust and the total thrust. The air supply is furnished by two Allison 1720 supercharger compressors driven by 150 HP Ford industrial engines, which are part of the Hiller air supply facility. The converter consists of a rotary valve and four jet tubes connected to the ports. A small, variable speed electric motor drives the valve. The airflow rate through the converter is

measured by means of a sharp-edged orifice, manometer, and a thermocouple in the supply pipe.

The relationship among the various valve and port dimensions which determines the open duration to cyclic period is shown in Figure 14. Operation of typical converter valve configurations is depicted in Figure 15. The converter geometry designated as "Model A" is the one which was tested and the results of this test are shown in Figure 16.

The primary intermittent jet tubes leading from the valve ports were 28-1/2" long by 1-1/8" diameter with about a 1/16" flare at the end. Thrust augmenter dimensions were 8" long by 1-3/4" throat, 8° divergent and were spaced 1-3/8" from the intermittent jet outlet. Valve rpm for tube resonance without augmenters was approximately 3800 rpm. With augmenters in place, valve rpm was reduced to approximately 3550 rpm for resonance. It was noted that maximum total thrust and maximum augmenter thrust occurred at slightly different rpm (difference of approximately 200), maximum total thrust occurring at the lower rpm.

Test data was taken for four different supply pressures, with augmenters and without. The data was reduced to the following quantities:

a. P/p_o, (atmospheric pressure)/(supply pressure)

b. Thrust, augmented and unaugmented

c. Augmentation ratios:

$\emptyset$ = (total thrust with augmenters)/(primary intermittent jet thrust without augmenters)

U = (total thrust with augmenters)/(primary intermittent jet thrust in presence of augmenters). The presence of augmenters affects the performance of the primary jet.

$\emptyset_s$ = (total thrust with augmenters)/(thrust which would be produced by the isentropic expansion of the measured flow rate of air from the supplied total pressure and temperature to ambient pressure or more simply, steady flow isentropic thrust).

d. Conversion efficiency = (thrust unaugmented)/(steady flow isentropic thrust).

e. Specific thrust = (thrust)/(primary jet air flow rate).

Corrections to standard conditions were not made.

The most interesting observations are that the conversion efficiency increases with increasing supply pressure. (By chopping 2-1/2" from the ends of the jet tubes and thus removing the end flare, the conversion efficiency was later increased from the maximum of 0.81 shown in Figure 16 to 0.91.) This rising trend of conversion efficiency is encouraging in view of the rising trend of the specific thrust curve. The isentropic augmentation ratio, ϕ_s, remains fairly constant over the pressure range investigated as does the total-to-primary jet thrust ratio. The augmenters contributed about one third of the total thrust; however, their presence affected the primary jet thrust adversely at high supply pressures and favorably at low supply pressures.

It is felt that the converter configuration and augmenter tuning or matching were not optimum in this initial test. Considerable gains in the conversion efficiency and isentropic augmentation ratio can probably be achieved with a valve geometry which would give a shorter open time to cyclic period ratio. Increases in specific thrust are also possible through increased thrust performance and higher supply pressures.

3. ANALYTICAL RESEARCH

3.1 Identification of Phenomena

Schlieren observations and high-speed pressure instrumentation both reveal that the pressure waves associated with the intermittent jet blow-down are of the N-wave type as sketched below:

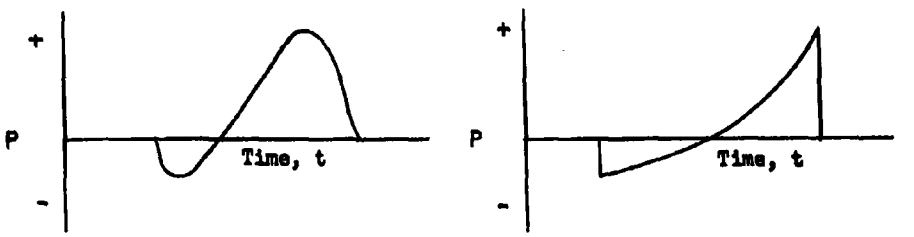

FIGURE E

This is basically a compression wave followed closely by, in fact coupled with, a rarefaction. It is also typical, for example, of spherical detonation waves (Ref. 13, pg. 660) and of the waves associated with the "sonic boom" emanating from high-speed aircraft. Further information on waves of this general type may be found in Reference 14, pg 168 and in section 158, pg 416, on blast waves. The fact that a following rarefaction wave will overtake and weaken a compression wave traveling into undisturbed fluid also explains why the fluid motion caused by the reciprocating motion of a piston in a tube is damped when the tube length exceeds a certain minimum length. This is true for the case in water as well as in gases.

The schlieren streak photograph records and pressure records indicate the presence of multiple N-waves during each cycle. This appears to be the case with the waves created by both the combustion-driven devices (pulsejets) and the mechanical converter. When these spherical N-waves strike the inlet of the thrust augmenter, a segment of the wave enters the augmenter tube essentially as a plane N-wave, or, to state it more precisely, as a band of plane N-waves. The N-waves, as created by the devices tested up to this time, are mildly predominated by the compression portion

of the N-waves, so they tend to reflect from the open aft end of the augmenter tube predominantly as rarefaction waves. Since these reflected rarefaction waves are travelling in a direction opposite that of the fluid that was induced to flow through the tube by the compression waves, the rarefaction waves also accelerate the fluid.

The importance of not neglecting the wave processes is substantiated by correlation between the experimental schlieren record of fluid and wave velocities and the high-speed pressure transducer records on one hand (figs. 17 and 18) with unsteady one-dimensional gas dynamic analysis (fig. 18b) on the other. That very large errors may be introduced into an analysis if steady-flow concepts and equations are used is indicated in the comparison (ref. 3, fig. 23) of pressure ratios associated with (a) a steady-flow isentropic process and (b) an isentropic wave process. This comparison shows that pressure ratio increments of as much as 2-1/2 times that found in the case of steady flow of the same fluid velocities (U = 0.4 to 0.8) may be achieved by wave processes.

Although it was recognized in the earlier studies (refs. 1 and 2) that the method of energy transfer in the intermittent jet thrust augmenter was quite different from the steady flow jet ejector (since it worked well when much too short for the typical steady-flow turbulent jet mixing process to occur), the method was not yet known. The unsteady jet augmenter also defied steady-flow ejector design rules by exhibiting optimum area ratios for maximum thrust augmentation at very small values such as 4:1, rather than showing continually increasing improvement with increase in the ratio of augmenter throat to jet outlet area. When these observations were combined, and thrust augmentation compared with that for steady flow jet ejectors, the result was much higher thrust augmentation with much smaller length-to-diameter ratios and area ratios. It was readily apparent that intermittent jet ejectors utilize a much more efficient process than do steady-flow jet ejectors. It was then postulated that the energy transfer occurred primarily as a pressure wave process. This could account for the high performance with very short augmenter lengths.

The fact that the augmenter-to-primary-jet cross-sectional area ratio generally optimizes at relatively small values, in the vicinity of 4:1, cannot be explained exclusively in terms of a wave process, but when it is considered in terms of the piston-like jet whose motion is induced by the waves, then it is much more understandable. High-speed motion pictures show that for an optimum area ratio there is a tight seal between the "jet piston" and the augmenter walls, even to the extent of some momentary spill-over of the jet over the augmenter lip as the jet piston enters (see sketch, fig. 1) but this spill-over fluid is later sucked back into the augmenter along with secondary fluid. Tests have shown that thrust augmentation decreases rapidly as the augmenter diameter is reduced below the optimum, causing excessive jet spill-over and choking of the primary jet flow through the augmenter tube. When the augmenter is larger in diameter than optimum, thrust drops off because the pressure seal between the jet piston and the augmenter walls cannot be maintained. The motion of the jet piston is associated with a complicated family of compression and rarefaction waves which appear to originate from the jet piston, reflect from it, and in some cases, probably are transmitted through it.

3.2 Analysis by Method of Characteristics and Wave Diagrams

As presented and discussed previously in Reference 3, Section 5.2, the basic equations of unsteady, one-dimensional gas dynamics are non-linear partial differential equations which in general, cannot be solved directly. However, there are techniques which use (a) purely numerical analysis, (b) graphical-numerical analysis and (c) purely graphical analysis to solve these difficult equations. The classical analysis (e.g., see Ref. 6) is based on the concept of the Riemann variables, the right-running P-waves and the left-running Q-waves, and uses the method of computation generally known as the "method of characteristics" to get solutions by means of wave diagrams, which are non-dimensional (time-distance) plots of these waves, and of the fluid velocity.

The following symbols are used in this analysis:

t.....time

τ.....dimensionless time $a_o t/L_o$

x.....distance coordinate

ξ.....dimensionless distance x/L_o

a,c.....velocity of sound

u.....fluid velocity

U.....dimensionless fluid velocity u/a_o

A.....dimensionless velocity of sound a/a_o

P.....U + A

Q.....U - A

s.....specific entropy

γ.....ratio of specific heats

R.....gas constant

S.....non-dimensional entropy $s/\gamma R$

L.....length

Subscripts

o.....reference condition

e.....conditions at end of duct

E.....conditions in fluid surrounding duct ends

The method of characteristics, which is taken from the theory of partial differential equations, is developed from the following facts:

In a non-dimensional plot of time versus distance, τ versus ξ,

$$\tau = \frac{a_o}{L_o} t \text{ and } \xi = \frac{x}{L_o} \quad \text{(following Rudinger, ref. 6)}$$

$\frac{d\xi}{d\tau} = U + A$ for P-waves

$\frac{d\xi}{d\tau} = U - A$ for Q-waves

$\frac{d\xi}{d\tau} = U$ for S

where $S = \frac{s}{\gamma R}$; $U = \frac{u}{a_o}$; $A = \frac{a}{a_o}$

These three curves are called "characteristic" curves, or "characteristics" of the basic partial differential equations and the wave diagram is also called a characteristic diagram. The curves of direction U are the paths of fluid elements. (U + A) and (U - A) represent the speeds of propagation

of disturbances or "signals" relative to the walls of the duct.

The pertinent conditions that exist at inlet and exit ends of the augmenter tube and within the tube will be briefly described in terms of these wave or characteristic diagrams, and reference made to other writings for more detailed discussion.

3.2.1 Inflow

Inflow, according to the schlieren frame and streak photography, occurs almost without exception only at the upstream or inlet end of the augmenter tube, i.e., there has been essentially no periodic flow reversal at the augmenter exit end.

The nonsteady isentropic inflow is treated as a quasi-steady process which gives the energy equation in the form

$$A_e^2 + \frac{\gamma-1}{2} U_e^2 = \left(A_E^o\right)^2$$

where A_E^o is the non-dimensional speed of sound at the stagnation temperature T_E^o of the fluid that is induced into the tube inlet. Subscript e refers to conditions at the tube ends, and subscript E refers to conditions in the fluid surrounding the tube ends. Further, following Foa (Ref. 9, pp 106-115)

$$\frac{\gamma+1}{4}\left(P_e^2 + Q_e^2\right) - \frac{3-\gamma}{2} P_e Q_e = \frac{4}{\gamma-1}\left(A_e^o\right)^2$$

whence $$\frac{P_e}{A_E^o} = \frac{3-\gamma}{\gamma+1}\frac{Q_e}{A_E^o} \pm \frac{4}{\gamma+1}\left[\frac{\gamma+1}{\gamma-1} - \frac{\gamma-1}{2}\left(\frac{Q_e}{A_E^o}\right)^2\right]^{1/2}$$

and there is a similar relationship for $\frac{Q_e}{A_E^o}$ in terms of $\frac{P_e}{A_E^o}$.

It should be noted that these two preceding equations apply to non-isentropic inflow as well, but their application to non-isentropic inflow usually requires an iterative procedure.

For convenience Foa presents these relationships as his Figures 6d-6,7,8 which are plots of P_e/A_E^o vs Q_e/A_E^o for values of γ of 5/3, 7/5 and 9/7. Rudinger (Ref. 6, pp 63-68) presents the same fundamentals in a somewhat different form noting that the boundary conditions required for

inflow are $U_e^2 + \frac{2}{\gamma-1} A_e^2 = \frac{2}{\gamma-1} A_E^2$

and $S_e = S_E$ where S is the non-dimensional form of the entropy, i.e., defined as $S = \frac{s}{c_p(\gamma-1)} = \frac{s}{\gamma R}$

where s is the specific entropy.

The first of the two boundary condition relations is combined with the basic Riemannian relationships:

$$P_e = \frac{2}{\gamma-1} A_e + U_e \text{ and } Q_e = \frac{2}{\gamma-1} A_e - U_e$$

to give the quadratic equation for A_e

$$A_e = \frac{P_e \text{ (or } Q_e) + \sqrt{\frac{\gamma-1}{\gamma-1} A_E^2 - \frac{\gamma-1}{2} P_e^2 \text{ (or } Q_e^2)}}{\frac{\gamma+1}{\gamma-1}}$$

For convenience Rudinger has plotted A_e/A_E versus P_e (or Q_e)$/A_E$ as his charts 1a, b, c in his Chapter XI.

If one decides to use the helpful orthogonal graphical inter-relationships between the physical plane ($A_o t/l_o$ versus x/l_o) and state plane (a/a_o versus u/a_o) as presented by Shapiro (Ref. 5,e.g., pg 939) it is convenient to note that the preceding isentropic relationship between stagnation conditions in the surrounding fluid and the conditions for inflow at the tube inlet are expressed (following Shapiro, pg 936) as the equation of the steady-state ellipse

$$\left(\frac{a_e}{a_o}\right)^2 + \frac{\gamma-1}{2}\left(\frac{u_e}{a_o}\right)^2 = \left(\frac{a_E}{a_o}\right)^2$$

as plotted in the state plane, and the P-waves and Q-waves intersect this elliptical line to define conditions both prior to and following passage of the waves. Intermediate states lie along these straight lines that define the P-and Q-waves.

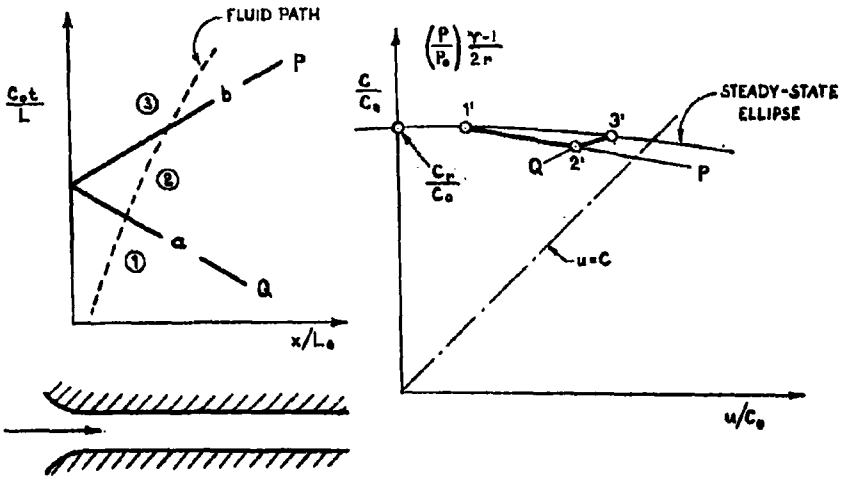

FIGURE F

For example, Figure F shows inflow to state 1' at the open end of the duct with a rarefaction wave approaching the open end from the right. Point 1' is located on the steady-state ellipse from the initial fluid velocity and point 2' is determined by the strength of wave a. In order to maintain the condition that all inflow states of the duct inlet must lie on the ellipse, wave b must be reflected as a wave of opposite kind, if the inflow is subsonic. State 3' may be located in the state plane, using the foregoing boundary condition and the additional condition that fields 2 and 3 lie on a common Q-characteristic. It should be noted that a region or area of the physical plane (t vs x) transposes into a single point on the state plane.

3.2.2 Outflow

When outflow is subsonic the key relationship is that $P_e = P_o = P_E$ where subscript e refers to the exit plane of the tube and subscript E refers to the outer region surrounding the tube.

since $\frac{P_e}{P_E} = \frac{P_e}{P_o} = 1.00 = A_e^7$ then $A_e = 1.00$

so $P_e = \frac{2}{\gamma-1}(1.00) + U_e$

and $Q = \frac{2}{\gamma-1}(1.00) - U_e$

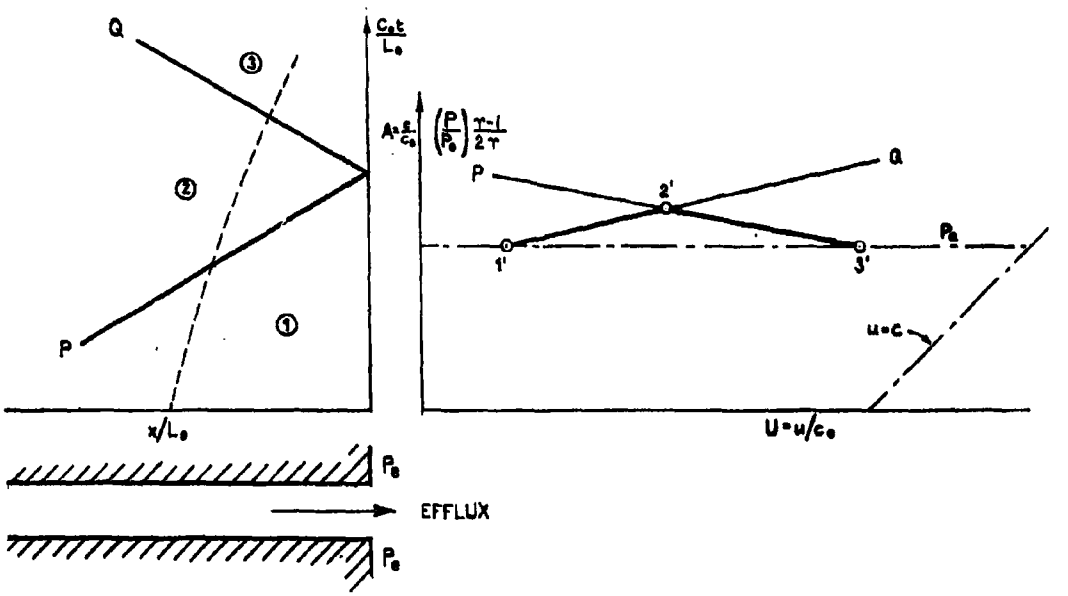

FIGURE G

Figure G indicates how a wave is reflected from a constant-pressure end as a wave of opposite kind (unlike sense). In this case a compression wave reflects as a rarefaction wave and both waves accelerate the fluid. At other positions inside the tube, the basic relationships hold that define P and Q-waves in terms of γ, A, and U and the following are useful:

$$A = \frac{\gamma-1}{4}(P + Q); \quad U = \frac{(P - Q)}{2}$$

In interpretation of the schlieren photos the intersection of opposite traveling waves yields important information, e.g.,

let $u + a = 1500$ fps

and $\underline{u - a = 400}$ fps

then $2u = 1100$ so $u = 550$ fps.

Given u and a, the magnitudes of both P and Q can be determined and their directions of propagation, since the direction of the P-wave is

$$\frac{a+u}{a_o} = A + U$$

and the direction of the Q-wave is $\frac{a-u}{a_o} = A - U$

on a plot of $\left(\frac{a_o}{L_o}\right) t$ versus $\frac{x}{L_o}$.

3.2.3 Wave Interaction with the Interface between the Jet Piston and Secondary Fluid

The schlieren record generally fails to reveal evidence of any waves crossing the interface between the driving and the driven fluid. It may be that the effects on the schlieren record of the hot, turbulent gases in the primary jet or driving fluid conceal waves that cross the interface. Method of characteristics analysis tabulated in Fig. 21a of the schlieren record of Fig. 21 was made on the assumption that right-running compression and rarefaction waves produced the changes of velocity (accelerations and decelerations) that were recorded. The same waves would have been produced ahead of the interface if the interface had been considered as a jet piston, whose changes of motion produced the waves, but the waves from the back side of the jet piston would have been waves of opposite kind. In the example of simplified analysis in Figure 18c using the Vector Polar Method, the interface has been considered as a jet piston moving at constant velocity.

Techniques for handling the interaction of waves with a plane discontinuity consisting of a plane interface between portions of the same gas at two different temperatures, or of two different gases, are discussed in detail in References 5,6,7,8,13,14 and 15, so the techniques will not be discussed herein. It is believed that a good analysis of the entire cycle may be achieved by handling the initial passage of waves and fluid interface

through the augmenter as first described and as illustrated in Figures 18c or 21a, and then considering that no additional waves enter the augmenter so that only the momentum of gases in the tube continues to produce new waves. That is, the gases within the tube would be considered to act as a free piston during the "tail-off" portion of the cycle. Investigation of the accuracy of this assumption is considered appropriate for the succeeding phase of the program.

The effect of changes of duct area and techniques for handling that situation are also discussed in detail in the foregoing references. Foa's Figures 6e-2 to 6e-8 inclusive (Ref. 9) are particularly helpful in this regard.

3.3 The Vector-Polar Method for the Analysis of Wave Interaction Processes

A rather new and novel method called the Vector-Polar Method has proven of great value in analysis of shock wave interactions, particularly in the case of situations concerned with detonation waves. The method, where applicable, has a most important feature which is that it considers (Ref. 12) "only the results of wave interaction phenomena and produces, therefore, a solution which can be described as one "in-the-large". It holds true only after all the local interaction effects have died out and small amplitude waves have either collapsed into finite amplitude shocks or "degenerated" into isentropic rarefaction fans. In contrast to this, the usual solutions obtained by the use of the method of characteristics which inquires into the details of the interaction as they progress, represent solutions "in-the-small"." This vector-polar graphical method is based on a modification of diagrams using the state plane which are usually plots of c/c_o versus u/c_o or p/p_o versus u/c_o (e.g., see Ref. 5 Shapiro, pg 935 and Ref. 15 Oswatisch, sec. 3.28, pg 154). As noted in References 7 and 8 the modification consists of the use of the logarithm of pressure ratio (or of the local velocity of sound ratio) as the ordinate instead of the conventional linear scale. This modification, which at first thought might seem trivial, is really quite important because, as the innovators (Oppenheim, Stern, Laderman and Urtiew) explain, it "imparts to the hodograph plane a complete vectorial character, with logarithm of the pressure ratio (or of local velocity of sound ratio) appearing as a real component of the vector representing the change of state.

Thus, each subsequent state is obtained as a sum of vectors representing the changes brought about by discontinuities forming the initial boundaries of its regime in the space-time domain. It is of interest to note also that, since the entropy change is a weighted sum of the logarithms of pressure and velocity of sound ratios, the logarithmic coordinates are essentially components of an over-all entropy change ($\Delta s/R$)-particle velocity ($\frac{u}{a_o}$) hodograph". Thus, it is that solution of the inherently non-linear problem of wave interaction is obtained graphically by utilizing the vectorial character of the state diagram. "Each point on the diagram represents the end-point of a vector (whose initial point is at the origin of the coordinate system), which represents the change of state brought about by a given wave process. If there is any other wave propagating into the new state, the result of its action is accounted for simply by vector addition. For this purpose, one only has to know the so-called wave polars, that is, the loci of states attainable by a given wave process. They represent, as a rule, the compatibility conditions imposed by restrictions invoked by the principles of conservation of mass, momentum and energy". Derivations of equations and plots of the rarefaction, shock and steady flow polars are presented in reference 8, but because our working region is near the origin of these curves the shock and rarefaction polars for $\gamma = 1.4$ are replotted as figures 23 and 24 in this report to an expanded scale for greater accuracy and convenience.

Examples of the Vector-Polar Method applied to the intermittent jet thrust augmenter problem are shown in figures 18c and 25. The problem as handled in figure 18c has been restricted to the wave interactions ahead of the jet piston interface. It must be noted that the Vector-Polar Method is to be used only in cases where complicated wave trains may be satisfactorily approximated by simple wave configurations with definite states between in order to reap the advantage of dealing with the process "in the large". In this particular case the accelerating interface is approximated by a constant velocity piston which enables us to take only one weak shock wave instead of a continuous compression fan. If a more accurate analysis is

to be performed, consideration must be given to the whole compression fans and rarefaction fans which are being continuously formed by an accelerating and decelerating piston, as revealed by the schlieren record of the motion of the jet piston interface. However, it should be noted that even the greatly simplified model shows the main features of the flow and gives a fair approximation to the pressure history as revealed by the high-speed pressure transducer record of Figure 18b. Since a paper is in preparation (ref. 12) that will describe in detail how to use the Vector-Polar Method, no further description will be given here. The Vector-Polar diagrams of Figures 18c and 25 were prepared by Paul Urtiew with advice from Drs. Laderman and Oppenheim. Figure 25 is discussed in the following section.

3.4 Possibilities of Improved Thrust Augmentation

It is believed that an even greater energy transfer and resultant thrust augmentation may be achieved by "tailoring" the waves that drive the primary jet piston. The following possibilities are suggested. The most promising augmenter shape is probably the divergent augmenter. Unlike the situation in the parallel-walled augmenter, a wave shape and pattern that created an average positive pressure in the divergent section would contribute to the augmenter thrust. In the case of current configurations the average pressure throughout the interior of the augmenter is negative, but the greater pressure drop on the lip of the divergent augmenters accounts for their superior thrust augmentation, as compared to the cylindrical type. In the proposed improvement, the relative frequency of the driving jet recurrence with respect to the natural frequency of the thrust augmenter tube would be increased so that the leading or head portion of the wave pattern would predominate, rather than the "tail-off" portion as in current combinations (see Figures 17-21 inclusive). Other features that may be utilized to increase the pressure differences that cause the augmenter thrust are: (a) the amount of negative gage pressure in a primary N-wave and also in waves that are reflected from an open end is obviously limited to one atmosphere (perfect vacuum), whereas much greater positive pressures are readily achieved. (b) Furthermore, wave reflection at both ends of the augmenter can be eliminated throughout much of

the cycle by sonic velocity of fluid.

The dimensionless time-distance graph on the upper right of figure 25 illustrates the idea of a hypothetical piston of infinitesimal thickness, which moves through the augmenter at constant velocity of such magnitude so as to maintain a rarefaction wave anchored at the augmenter inlet. The simplified analysis of the conditions specified uses the Vector-Polar Method as illustrated by the graph on the upper left of figure 25. The second dimensionless time-distance plot (lower right) is a modification of the foregoing conditions by specifying that a standing rarefaction wave also be anchored at the outlet of the augmenter. In order to accomplish this the idealized hypothetical jet piston is now considered to be an expanding (thickening) piston as indicated by the difference between states 1 and 1a on both the Vector-Polar and dimensionless time-distance diagrams. The pressure-time histories at several selected stations are shown in figure 25a, as well as a plot of pressure-impulse (pt) versus augmenter length. The latter plot shows how to locate the station (0.65L) at which the time-averaged pressure or pressure-impulse is zero. Forward of this station the average pressure is negative, whereas aft it is positive. This indicates that it is unwise, in this particular hypothetical case, to make the augmenter divergent between station 0 and station 0.65L because of the resultant loss of thrust that might occur in that region due to the occurrence of negative average pressure. This forward section may either be made convergent to take advantage of the negative average pressure or be made parallel-walled to prevent a loss of thrust in that section. On the other hand the pressure-impulse records suggest that an increase of thrust might be achieved by flaring the aft end of the augmenter to take advantage of the positive average pressure in that region. For the sake of simplification, the pressure-impulse distribution calculations shown in figure 25a were based on a cylindrical augmenter with flared inlet. Furthermore, the pressure due to passage of the N-wave across the inlet flare was ignored. Negative pressures on the inlet flare were calculated using a linear space distribution of pressure from maximum at the throat section

to zero gage pressure at the edge of the lip of the inlet flare. This resulted in a calculated thrust on the lip of 740 lbs. An additional thrust of approximately 80 lbs might be recovered by utilizing the positive average pressure on an aft flare of the augmenter outlet. Of course, the pressure distribution would actually be somewhat different due to the effect of the flared outlet as compared to the preceding calculations for a parallel-walled duct. These thrust values may be compared to a thrust of about 168 lbs on a tailpipe augmenter of similar size for a valveless pulsejet with tailpipe thrust of 120 lbs. However, the jet from the valveless pulsejet possesses much less kinetic energy than would a real jet with the high velocity characteristics of figure 25.

4. DISCUSSION OF CURRENT ACHIEVEMENTS AND ADDITIONAL WORK

The current program has produced greatly improved flow visualization through the intermittent jet augmenter as a result of the development of a multi-colored filter used in conjunction with the schlieren high speed color motion picture and streak photography. Instantaneous pressure measurements in the augmenter have been taken and a correlation has been made between these measurements and the theoretical analysis. A mechanical device for converting a steady flow into an intermittent jet without creating upstream disturbances has been tested and evaluated. This mechanical device for converting steady flow to intermittent jets is of particular importance for the following reasons:

(a) It has now been demonstrated that it is an excellent research tool for creating an intermittent jet without the added experimental and analytical complications of the combustion-driven jets (i.e., pulsejets), yet it can closely approximate the important characteristics of the latter.

(b) It permits a variation of such parameters as intermittent jet nozzle pressure ratio, jet blow-down velocity, and the ratio of blow-down to refill time.

(c) It appears to have real possibilities as a practical device for augmenting the thrust and reducing the downwash velocities and temperatures of steady flow jets by converting them to intermittent jets.

The analytical treatment has produced an insight into the dynamics of the fluid flow and has indicated the affect of augmenter parameters on performance. In general, there has been a rewarding increase in progress and understanding of this highly efficient energy transfer mechanism from primary (driving jets) to secondary flow.

In the continuing work this contractor would seek to refine the analysis of the intermittent jet energy transfer and to broaden the scope of understanding and experience to include variations of non-steady cyclic

forms as well as to continue to develop the measuring techniques for providing data to support the analysis. These areas of additional investigation can be defined as:

(a) Continue to develop and refine the theoretical analysis of the intermittent jet ejector.

(b) Continue investigation and application of pressure, temperature, and flow rate measuring techniques as well as flow visualization methods to provide data for support of the theoretical analysis.

(c) Further develop and make use of the device for converting a steady flow into an intermittent jet as a means for providing intermittent jets of various wave forms and velocities, and for determining the optimum jet wave form and velocity to provide the highest thrust augmentation and/or pumping performance possible.

(d) Consider and evaluate the use of high speed computer methods for investigating theoretically the effects of parameter changes to intermittent jet thrust augmenters.

5. REFERENCES

1. Lockwood, R. M.: "Proposal for Investigation of the Process of Energy Transfer from an Intermittent Jet to Ambient Fluid", Hiller Aircraft Corp. Report No. ARD-199, May 1958. (Limited copies -- available by direct request from Hiller Aircraft Company.)

2. Lockwood, R. M.: "Investigation of the Process of Energy Transfer from an Intermittent Jet to Ambient Fluid - Summary Report", Hiller Aircraft Corp. Report No. ARD-238, June 1959. Contract Nonr 2761(00). (ASTIA No. AD 233 349.)

3. Lockwood, R. M.: "Interim Summary Report on Investigation of the Process of Energy Transfer from an Intermittent Jet to Secondary Fluid in an Ejector-Type Thrust Augmenter", Hiller Aircraft Corp. Report No. ARD-286, 31 March 1961. Contract Nonr 3082(00). (ASTIA No. AD 265 071.)

4. Dean, Robert C.: "Aerodynamic Measurements", Gas Turbine Laboratory, Massachusetts Institute of Technology, The M.I.T. Press, Cambridge, Massachusetts, 1953.

5. Shapiro, Ascher H.: "The Dynamics and Thermodynamics of Compressible Fluid Flow", Vol. II, Ronald Press Co., New York, 1954, 534 pp.

6. Rudinger, George: "Wave Diagrams for Nonsteady Flow in Ducts", D. Van Nostrand Co., Inc., Princeton, N.J., 1955.

7. Oppenheim, A. K., and Stern, R. A.: "On the Development of Gaseous Detonation II. Analysis of Wave Interaction Phenomena", Technical Note DR 2, University of California, July, 1958 (AFOSR-TN-58-384; ASTIA AD No. 154 291.)

8. Oppenheim, A. K., and Urtiew, P. A.: "Vector Polar Method -- for Shock Interactions with Area Disturbances", Technical Note DR 4, University of California, July 1959 (AFOSR TN 59-701.)

9. Foa, J. V.: "Elements of Flight Propulsion", John Wiley and Sons, Inc., New York, 1960. (Dr. Foa is currently Professor of Aeronautical Engineering, Rensselaer Polytechnic Institute.)

10. Lockwood, R. M., Sargent, E. R., and Beckett, J. E.: "Thrust Augmented Intermittent Jet Lift-Propulsion System - 'Pulse Reactor'", Hiller Aircraft Corp. Report No. ARD-256, February 1960. Contract NOa(s)59-6055c.

11. Lockwood, R. M., and Patterson, W. G.: "Pulse Reactor Lift-Propulsion System Development Program - Interim Report", Hiller Aircraft Corp. Report No. ARD-301, December 1961. Contract NOw 61-0226c.

12. Oppenheim, A. K., Urtiew, P. A., and Laderman, A. J.: "Vector Polar Method for the Evaluation of Wave Interaction Processes", University of California, Berkeley. (Manuscript in preparation)

13. Kantrowitz, A.: "One-Dimensional Treatment of Nonsteady Gas Dynamics", High Speed Aerodynamics and Jet Propulsion, Vol. III, Princeton University Press, 1958.

14. Courant, R., Freidrichs, K. O.: "Supersonic Flow and Shock Waves", Interscience Publishers, New York, 1948.

15. Oswatitsch, K., Kuerti, G.: "Gas Dynamics", Academic Press, Inc., New York, 1956.

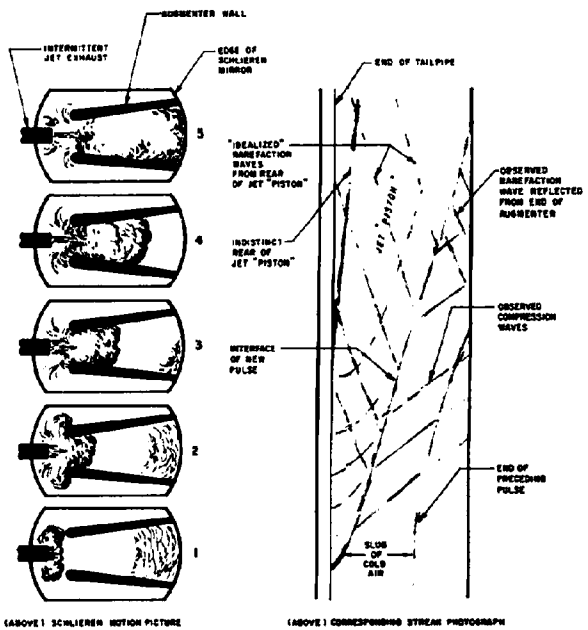

(ABOVE) SCHLIEREN MOTION PICTURE

(ABOVE) CORRESPONDING STREAK PHOTOGRAPH

FIGURE 1: REPRESENTATIVE SCHLIEREN INTERMITTENT FLOW VISUALIZATION

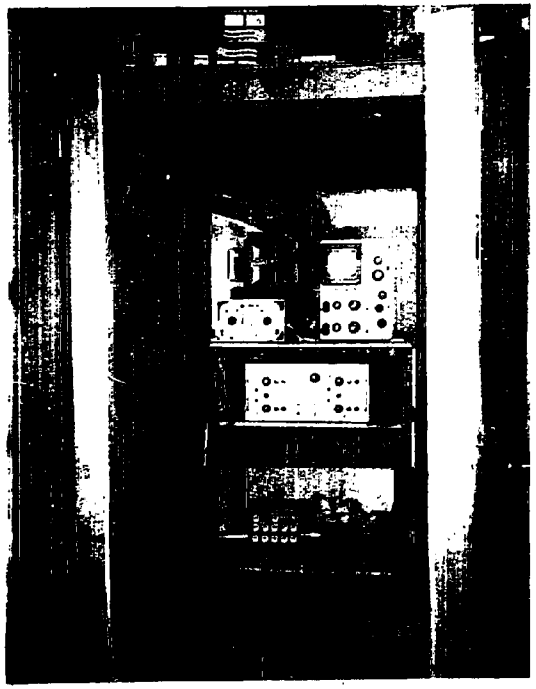

FIGURE 2: ACOUSTICAL ISOLATION CHAMBER FOR ELECTRONIC EQUIPMENT

FIGURE 3: OSCILLOSCOPE POLAROID PHOTOGRAPH DEMONSTRATING FOUR SIGNAL DISPLAY CAPABILITY

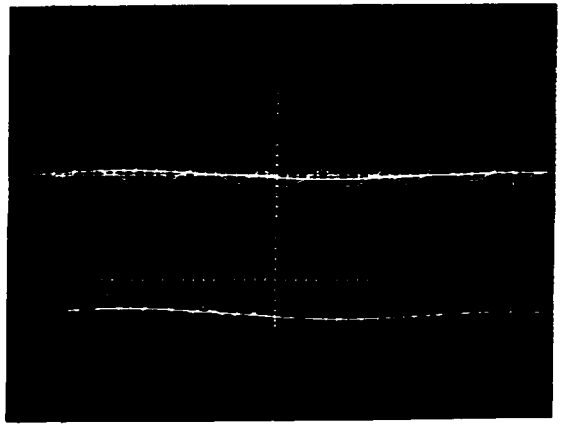

FIGURE 4: OSCILLOSCOPE POLAROID PHOTOGRAPH SHOWS MICROPHONICS IN ELECTRONIC EQUIPMENT CAUSED BY HIGH ACOUSTICAL NOISE ENVIRONMENT CREATED BY THE PULSEJET. SWEEP SPEED 2 MILLISECONDS/cm; VERTICAL AMPLIFICATION - CHARGE AMPLIFIER 50 mv/pcb, SCOPE 50 mv/cm.

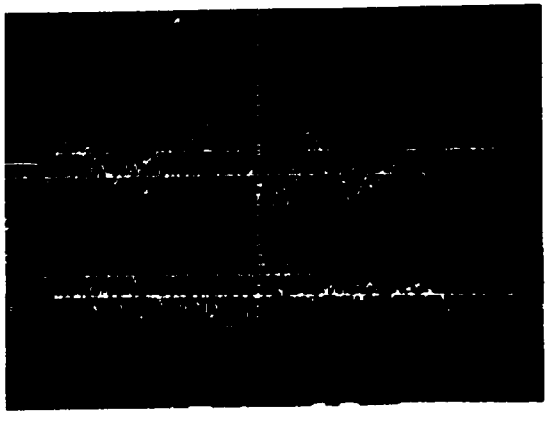

FIGURE 5: OSCILLOSCOPE POLAROID PHOTOGRAPH OF PRESSURE TRACES ILLUSTRATES SIGNAL NOISE DURING PULSEJET OPERATION ATTRIBUTED TO ACCELERATION VIBRATION RESPONSE OF KISTLER TRANSDUCER MOUNTED RIGIDLY IN AUGMENTER WALL. TOP TRACE FROM TRANSDUCER PRESSURE FACE MOUNTED FLUSH WITH AUGMENTER WALL. LOWER TRACE FROM TRANSDUCER MOUNTED IN BLIND HOLE. SWEEP SPEED 1 MILLISECOND/cm; VERTICAL AMPLIFICATION - CHARGE AMPLIFIER 20 mv/pcb, SCOPE 20mv/cm, OVER-ALL 1 pcb/cm OR APPROXIMATELY 2 psi/cm.

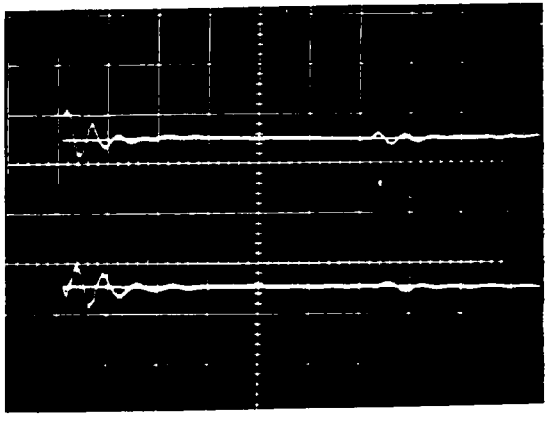

FIGURE 6: POLAROID PHOTOGRAPH OF PRESSURE TRACES ILLUSTRATE MECHANICAL RINGING OF AUGMENTER ASSEMBLY AND ACCELERATION RESPONSE OF KISTLER TRANSDUCERS. TRANSDUCERS MOUNTED IN AUGMENTER WALL WITH RUBBER "O" RING SEALS. DISTURBANCE CREATED BY TAPPING AUGMENTER ASSEMBLY WITH A SCREWDRIVER. SWEEP SPEED 2 MILLISECONDS/cm; VERTICAL AMPLIFICATION - CHARGE AMPLIFIERS 20 mv/pcb, SCOPE 20 mv/cm, OVERALL 1 pcb/cm.

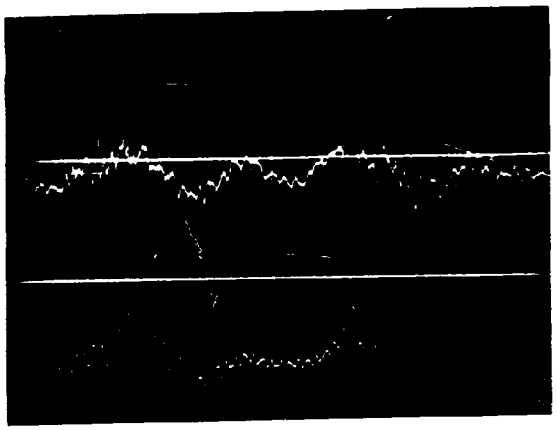

FIGURE 7: COMPARISON OF THE KISTLER AND C.E.C. TRANSDUCER'S SENSITIVITY TO ACCELERATION PRODUCED BY THE AUGMENTED PULSEJET. UPPER TRACE KISTLER TRANSDUCER, AMPLIFICATION APPROX 2 psi/cm; LOWER TRACE C.E.C. TRANSDUCER, AMPLIFICATION APPROX 3 psi/cm. SWEEP SPEED 1 msec/cm. BOTH TRANSDUCERS RIGIDLY MOUNTED IN AUGMENTER WALL.

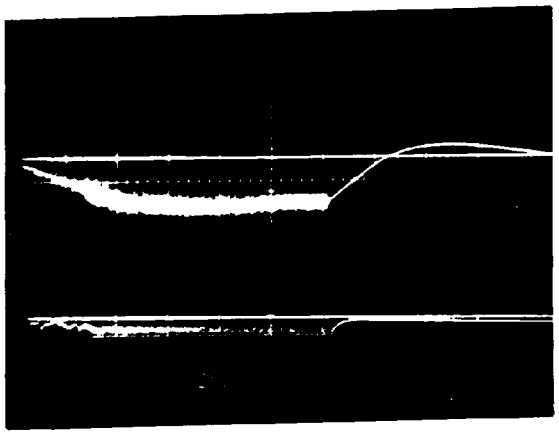

FIGURE 8: COMPARISON OF PRESSURE TRACES FROM KISTLER AND CEC TRANSDUCERS ILLUSTRATES THERMAL DRIFT OF EACH FROM BRIEF PERIOD OF PULSEJET OPERATION. UPPER TRACE FROM KISTLER TRANSDUCER: VERTICAL AMPLIFICATION - CHARGE AMPLIFIER 20 mv/pcb, SCOPE 50 mv/cm, OVER-ALL 2.5 pcb/cm OR APPROXIMATELY 5 psi/cm. LOWER TRACE FROM CEC TRANSDUCER: VERTICAL AMPLIFICATION - 10 mv/cm OR ABOUT 7.5 psi/cm. BOTH TRACES: SWEEP SPEED 0.5 sec/cm, DC COUPLING

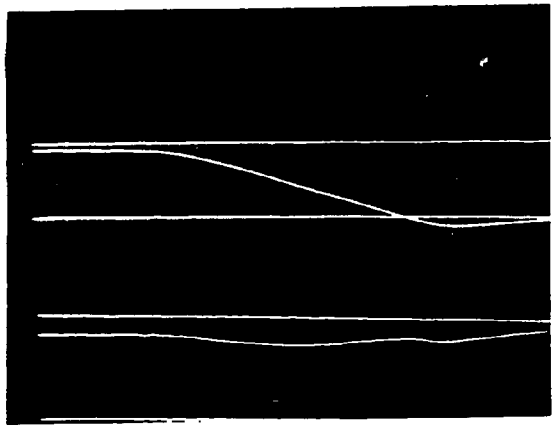

FIGURE 9: THERMAL SENSITIVITY OF KISTLER PRESSURE TRANSDUCERS. VERTICAL AMPLIFICATION: 1 pcb/cm. SWEEP SPEED 1 sec/cm. TOP TRACE IS UNCOOLED KISTLER. LOWER TRACE IS WATER COOLED KISTLER. BOTH TRANSDUCERS D-C COUPLED TO SCOPE. OBSERVE INSTABILITY (DRIFT) OF 0 PSIG REFERENCE LINES AS WELL AS THE THERMAL DRIFT CAUSED BY DIRECTING THE HOT AIR STREAM (ABOUT 250°F) FROM A "HAIR DRYER" ON THE TRANSDUCERS.

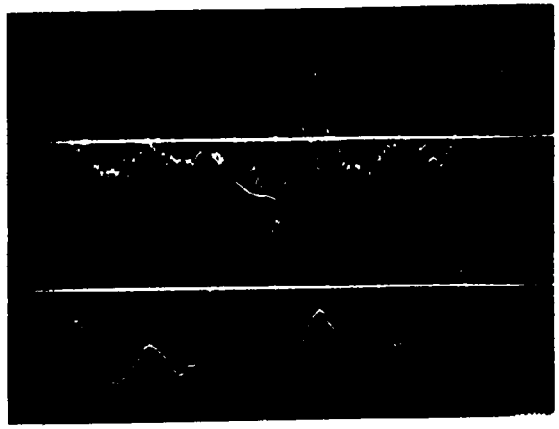

FIGURE 10: POLAROID PHOTOGRAPH OF PRESSURE TRACES FROM KISTLER TRANSDUCERS ILLUSTRATING REDUCED NOISE. UPPER TRACE FROM RIGIDLY MOUNTED TRANSDUCER, A-C COUPLING TO SCOPE. LOWER TRACE FROM LARGE MASS WATER COOLED ADAPTER SOFT MOUNTED WITH RUBBER "O" RING SEALS IN AUGMENTER WALL. D-C COUPLING TO SCOPE. SWEEP SPEED 1 MILLISECOND/cm. VERTICAL AMPLIFICATION: CHARGE AMPLIFIER 20 mv/pcb; SCOPE 20mv/cm; OVER-ALL 1 pcb/cm OR APPROXIMATELY 2 psi/cm.

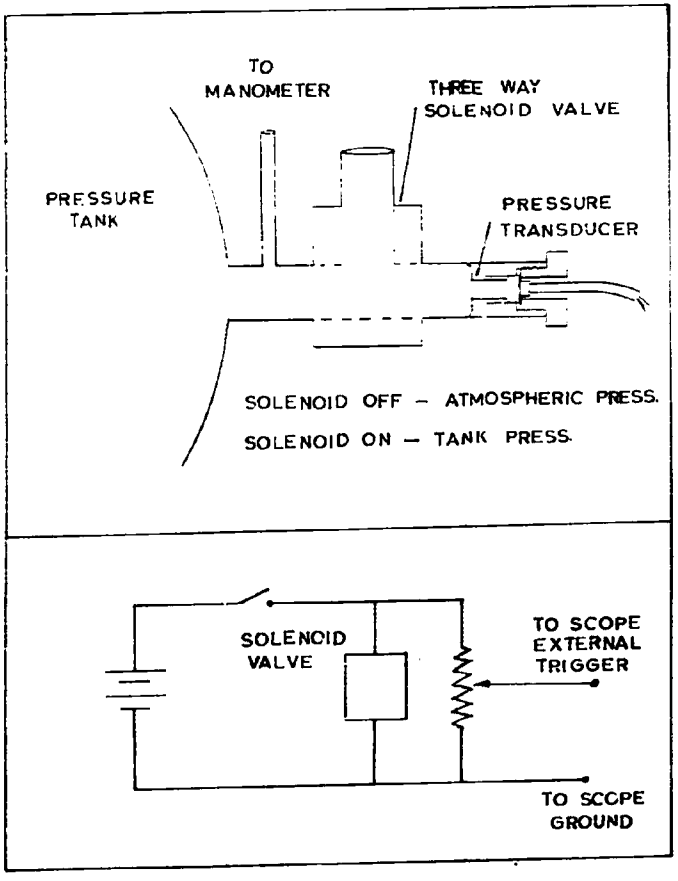

FIGURE 11: PRESSURE TRANSDUCER CALIBRATOR

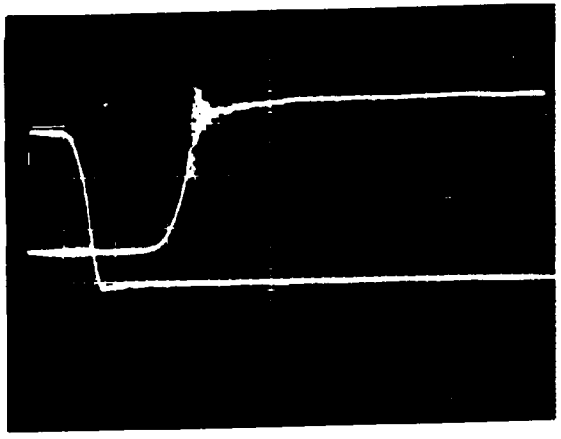

FIGURE 12: TRANSDUCER CALIBRATION
TANK PRESSURE 6.35 psig, CHARGE AMPLIFIER 20 mv/pcb, SCOPE AMPLIFIER 20 mv/cm, DC COUPLING, SWEEP 5 msec/cm. TRANSDUCER SENSITIVITY DETERMINED TO BE 0.45 pcb/psi.

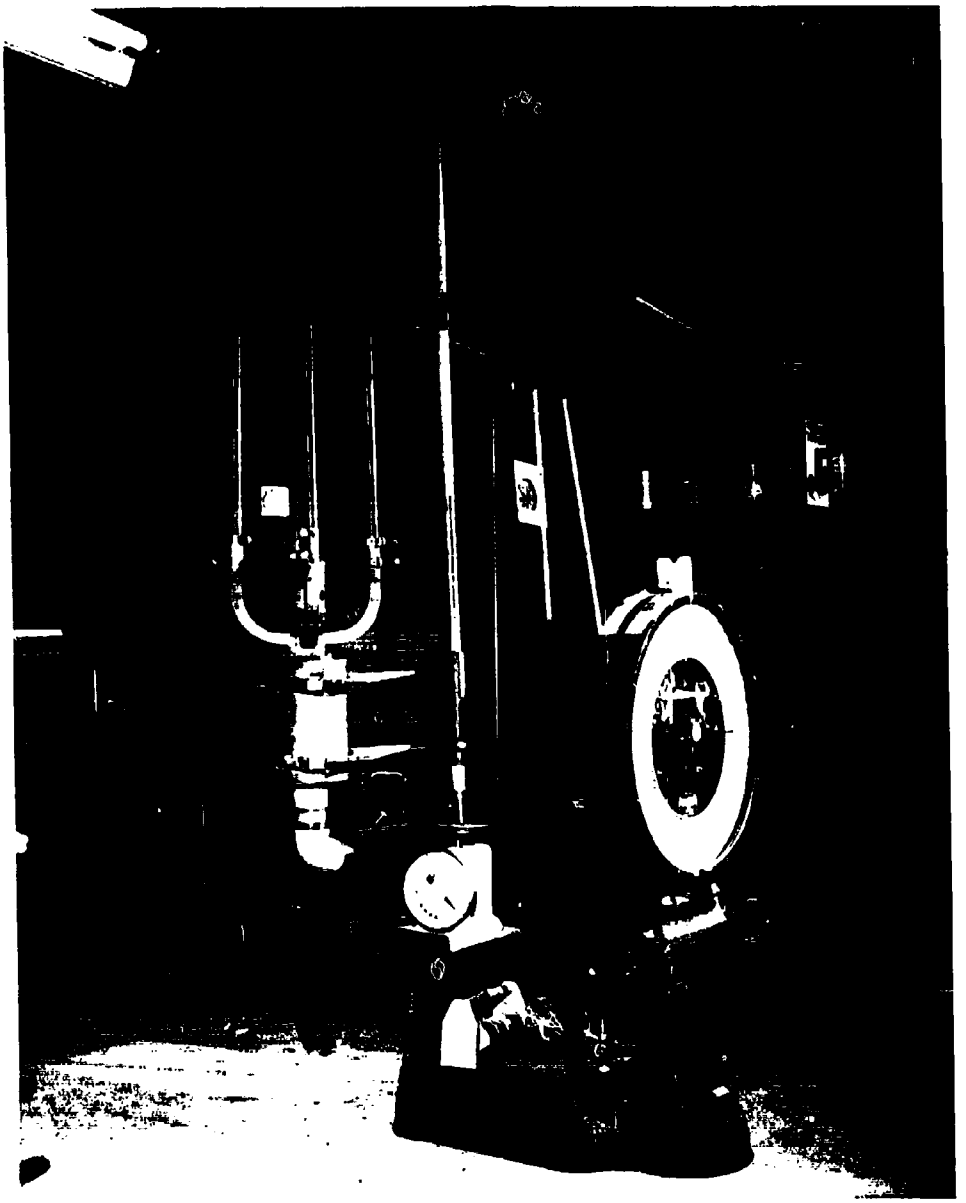

FIGURE 13: CONVERTER AND TEST SET-UP

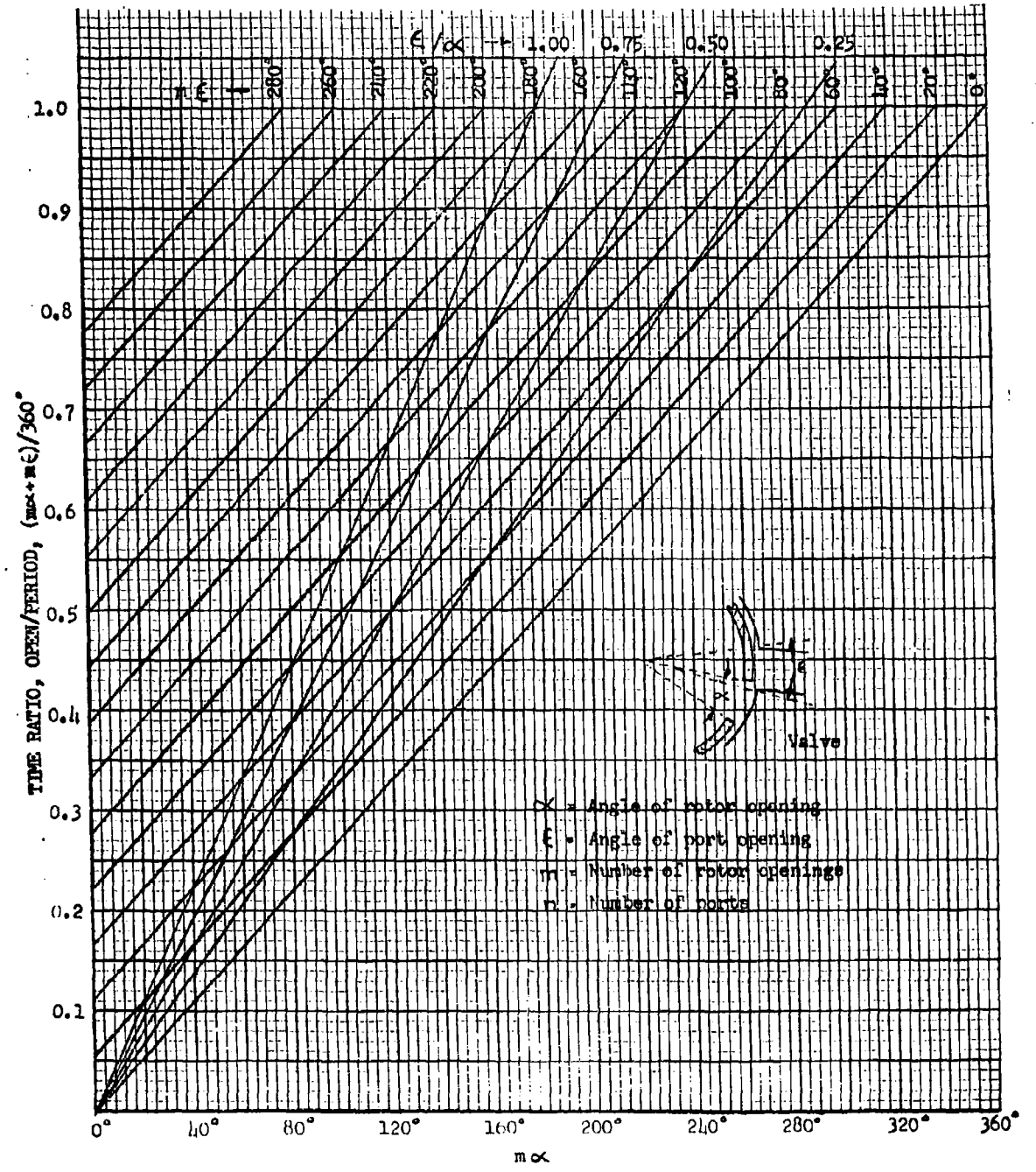

FIGURE 14: CONVERTER VALVE RELATIONSHIPS

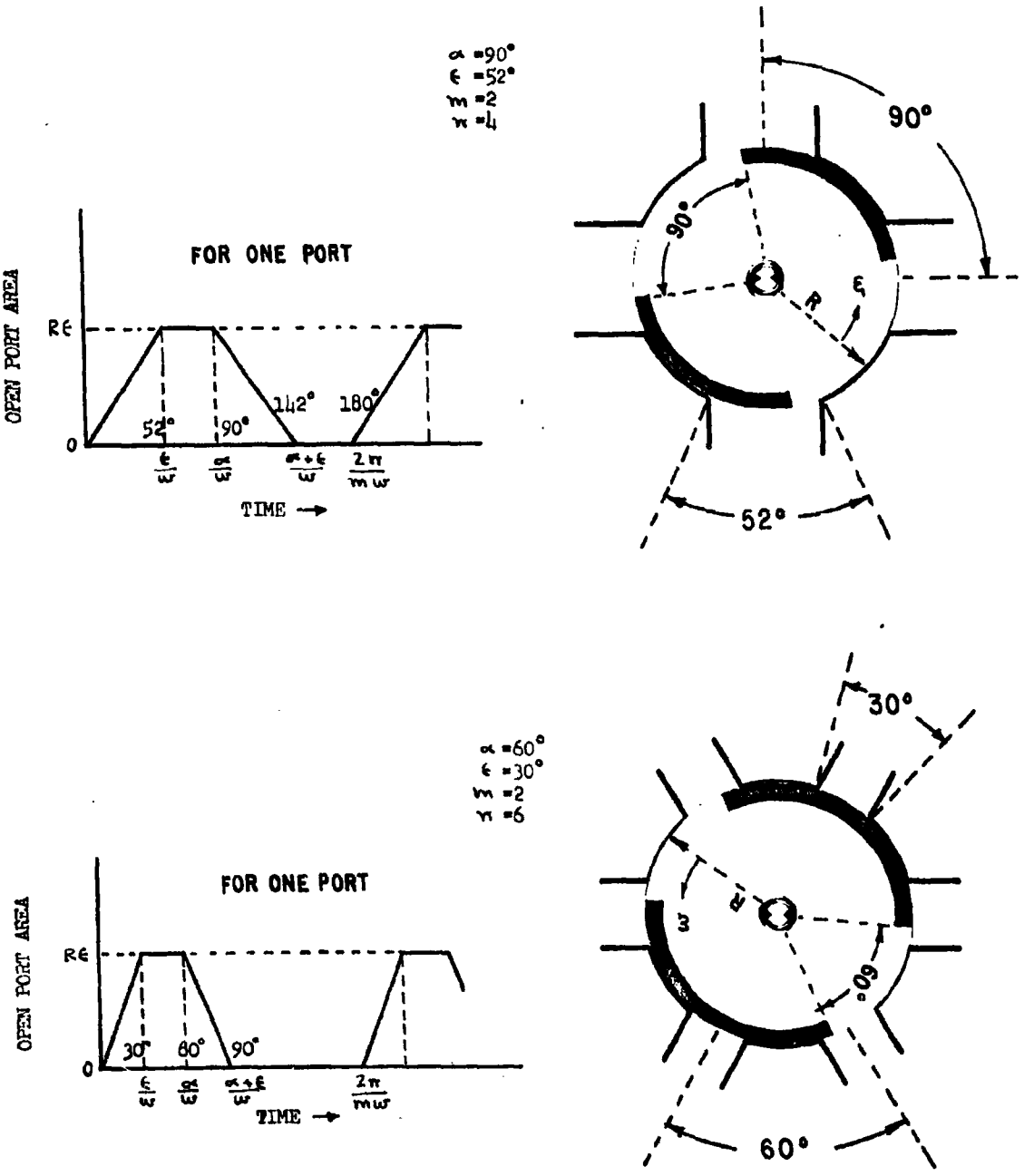

FIGURE 15 OPERATION OF TYPICAL CONVERTER VALVE CONFIGURATIONS

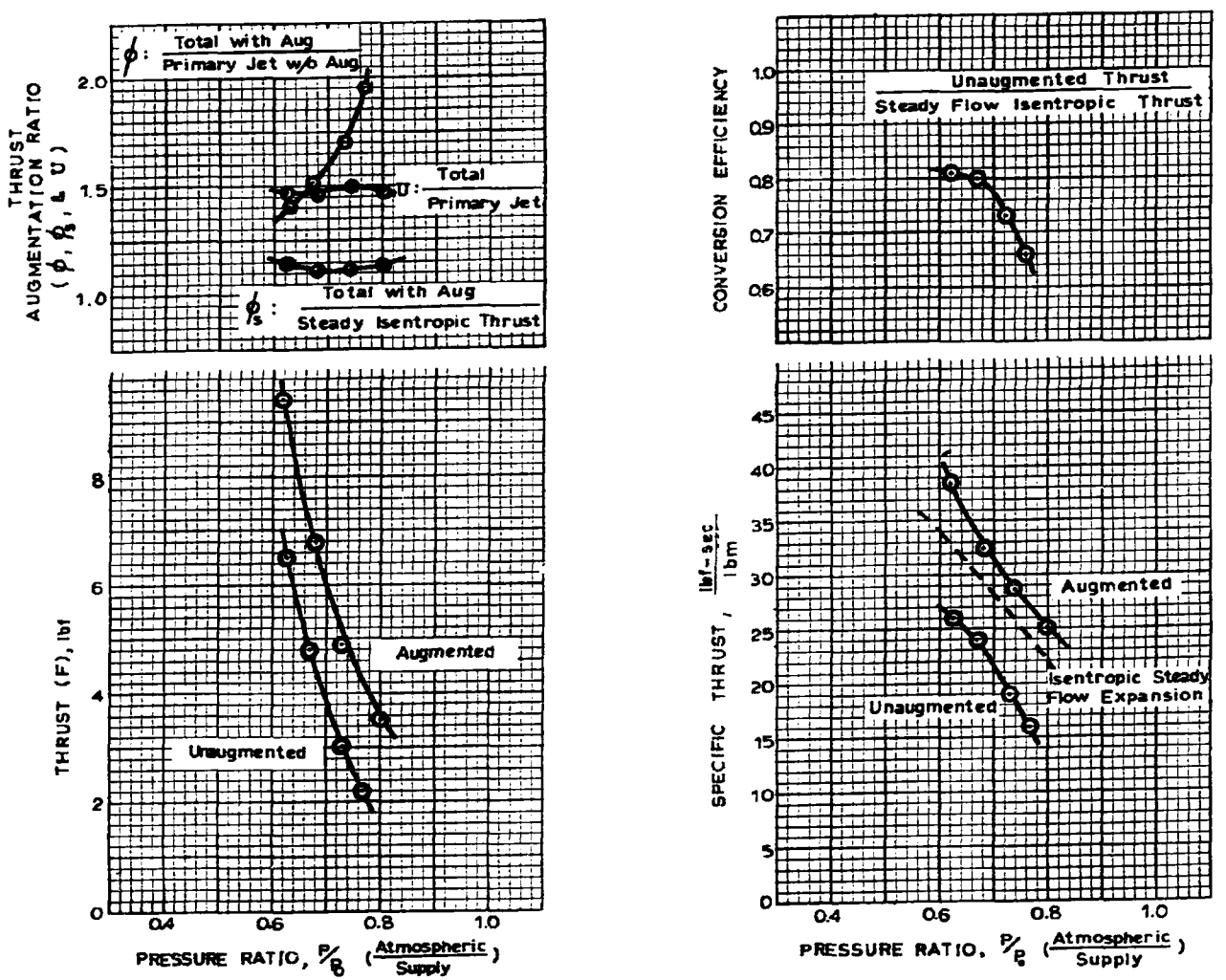

FIGURE 16: CONVERTER PERFORMANCE (MODEL A)

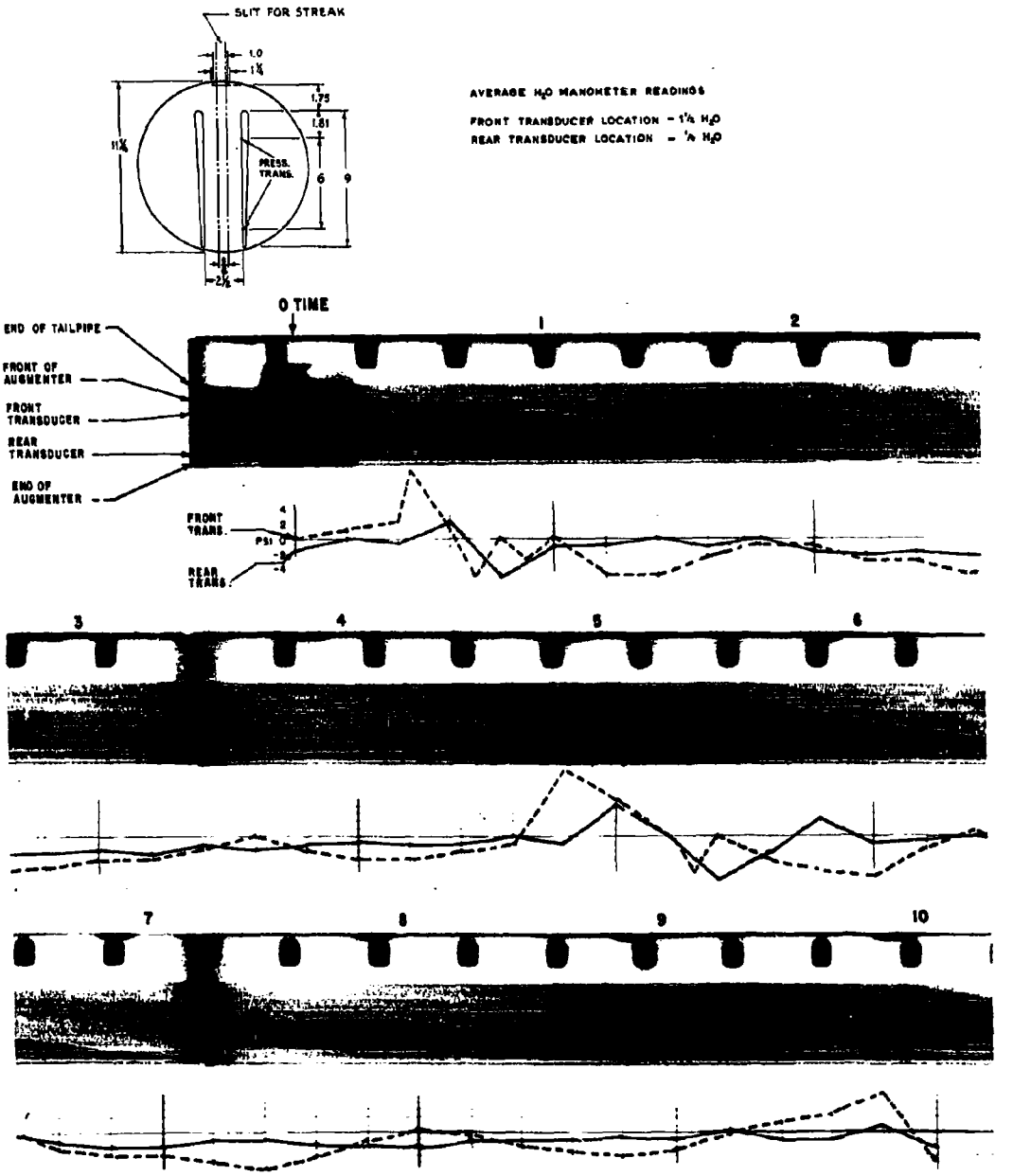

FIG.17 SCHLIEREN STREAK PHOTOGRAPHY AND ASSOCIATED PRESSURE RECORD FOR DYNAJET PULSEJET AND PARALLEL-WALLED AUGMENTOR [illegible]

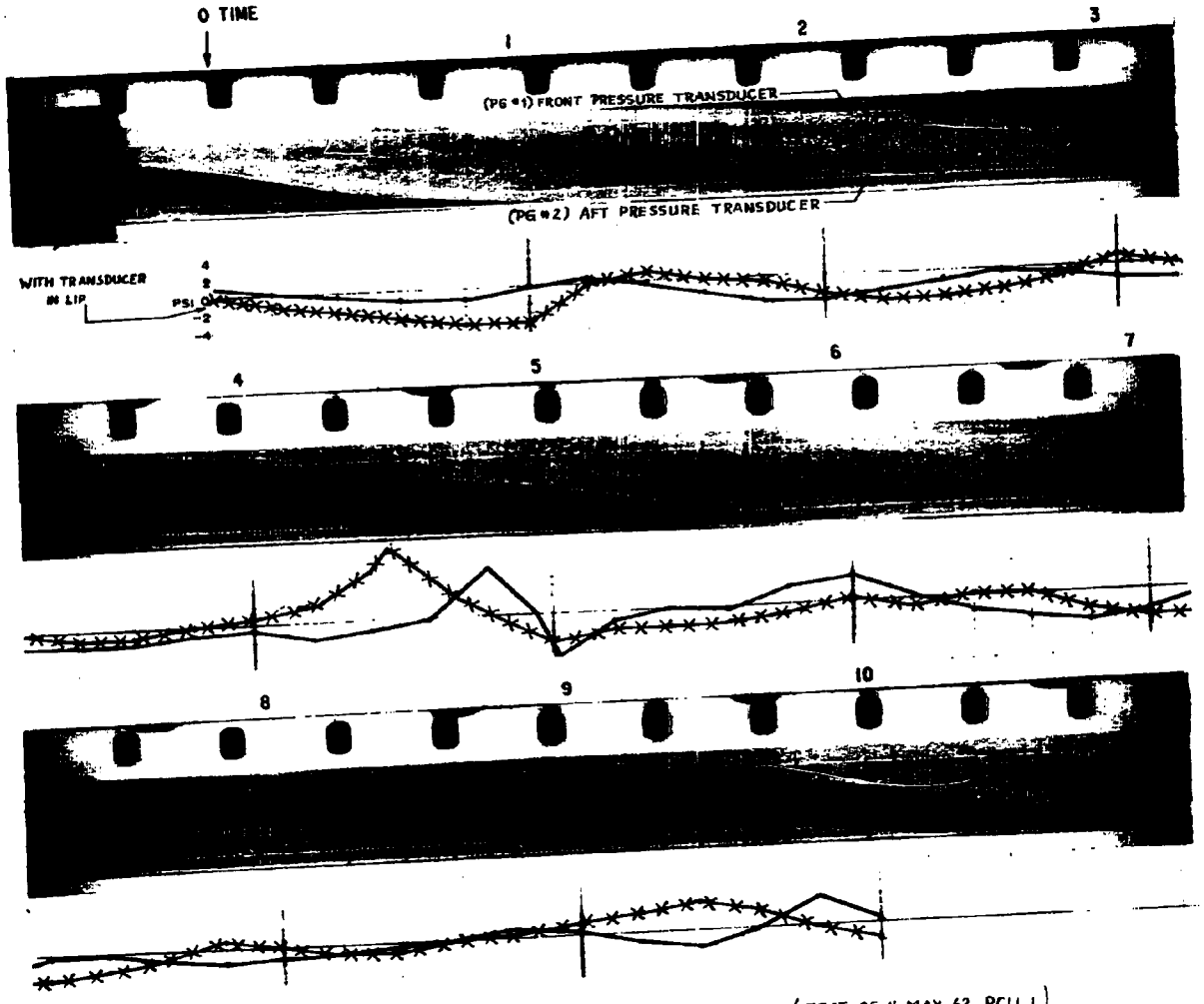

FIG. 18 TRANSDUCER ON LIP - DYNAJET WITH AUGMENTER 8° DIVERGENT (TEST OF 11 MAY 62, ROLL 1)

WAVE VELOCITIES

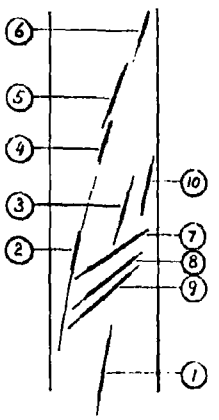

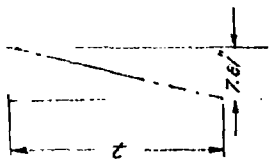

$$v = \frac{7.81''}{t} = \frac{7.81}{12}\,\frac{1}{t},\ \frac{ft}{sec}$$

$$= \frac{.65}{t}$$

No	t, ms	v, ft/sec
1	3.72	175
2	1.57	414
3	1.7	382
4	1.37	474
5	1.27	511
6	2.08	313
7	.38	1710
8	.41	1585
9	.43	1510
10	1.48	440

$u + a = 1710$

$u = 414$

$\therefore\ a = 1296$

$$a_o = a - \frac{\gamma-1}{2}u$$

$$= 1296 - .2\,(414)$$

$$\therefore\ a_o = 1213 \text{ ft/sec}$$

FIGURE 18a: KEY WAVE AND FLUID VELOCITIES FROM FIGURE 18

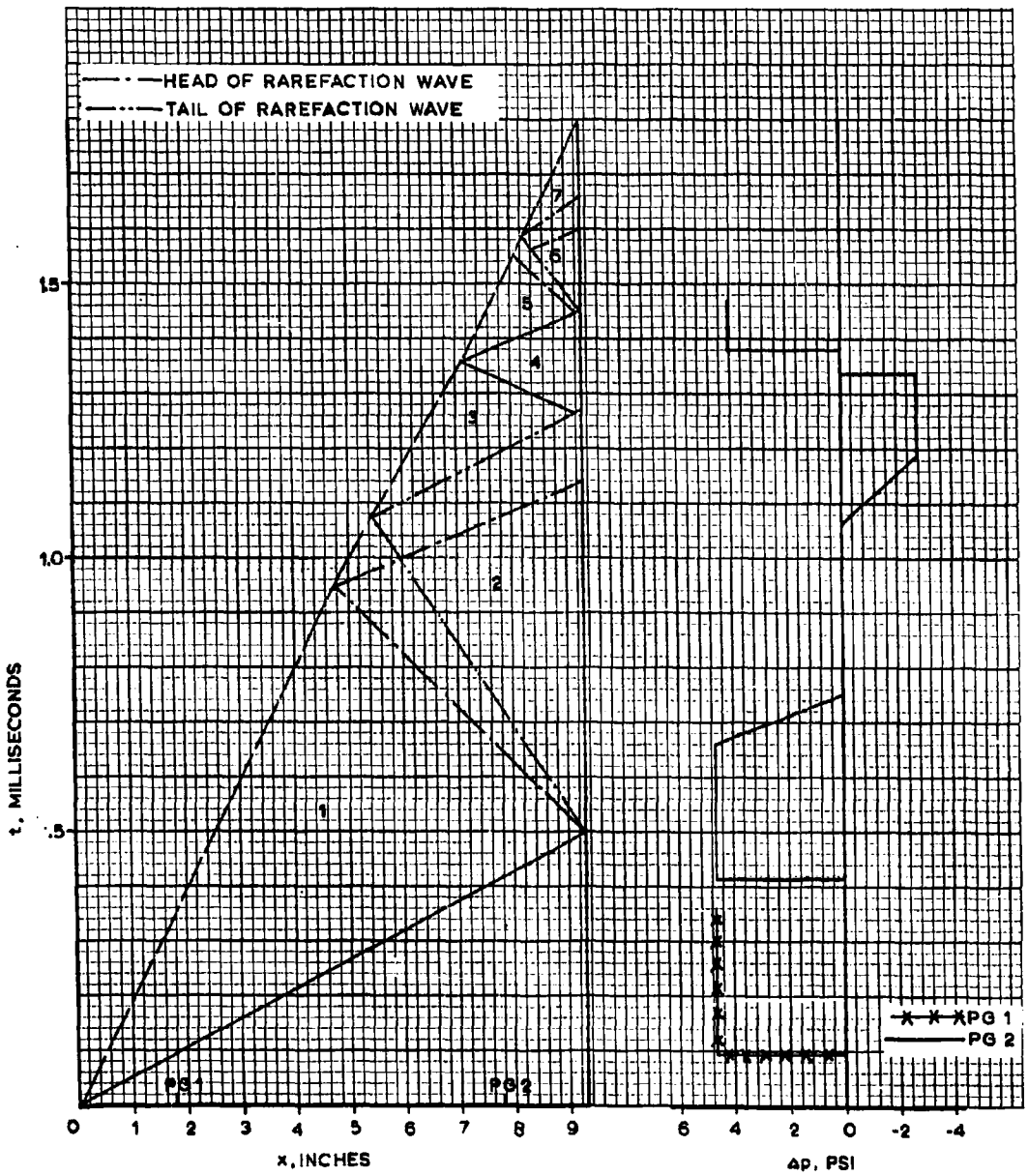

FIG. 18b: t-x AND t-Δp PLOTS OF SIMPLIFIED REPRESENTATION OF WAVE INTERACTIONS AHEAD OF JET PISTON IN THRUST AUGMENTER

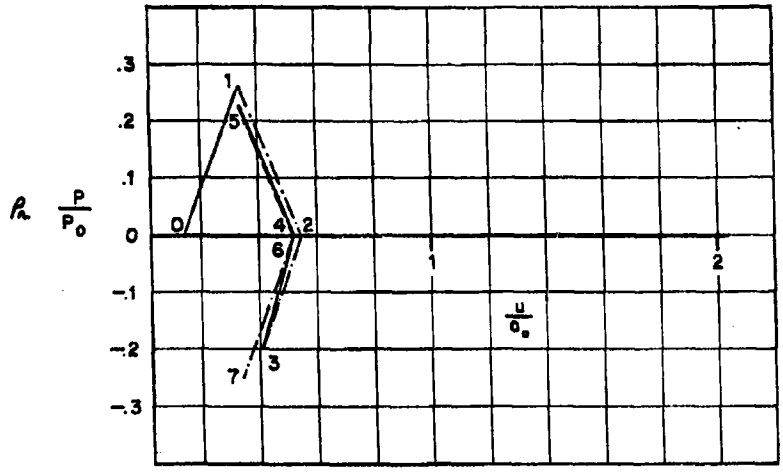

State Parameters

State	M	P	$\frac{p}{p_o}$	A	$\frac{a}{a_o}$	U	V	u+V	ΔP	u	u+v
									psi	ft/sec	ft/sec
0	0	0	1	0	1	.144	0	.144	0	175	175
1	1.13	.28	1.323	.04	1.04	.34	1.13	1.274	4.75	414	1555
2	$\frac{-1}{-1}$	-.28	1	-.04	1	.54	-1.04 -1.00	-.70 -.46	0	655	-850 -560
3	$\frac{1}{1}$	-.2	.808	-.03	.97	.4	1.00 .97	1.54 1.37	-2.65	487	1870 1660
4	1.08	.2	1	.03	1	.52	1.05	1.45	0	633	1770
5	1.11	.25	1.28	.036	1.036	.34	1.11	1.63	4.12	414	1980
6	$\frac{-1}{-1}$	-.25	1	-.036	1	.52	-1.036 -1.00	-.696 -.48	0	633	-846 -585
7	$\frac{1}{1}$	-.25	.78	-.036	.965	.34	1.00 .965	1.52 1.305	-3.24	414	1850 1580

Note: $M = \frac{v}{a}$ wave Mach No. relative to velocity of sound of the medium into which it propagates

$P = \ln \frac{p}{p}$ across one wave

$A = \ln \frac{a}{a}$ across one wave

$U = \frac{u}{a_o}$ dimensionless particle velocity

$V = \frac{v}{a_o}$ dimensionless wave velocity

$a_o = 1213$ (See Fig. 18a)

FIG. 18c: VECTOR POLAR ANALYSIS OF SIMPLIFIED (CONSTANT VELOCITY) JET PISTON-THRUST AUGMENTER WAVE INTERACTIONS AHEAD OF JET PISTON

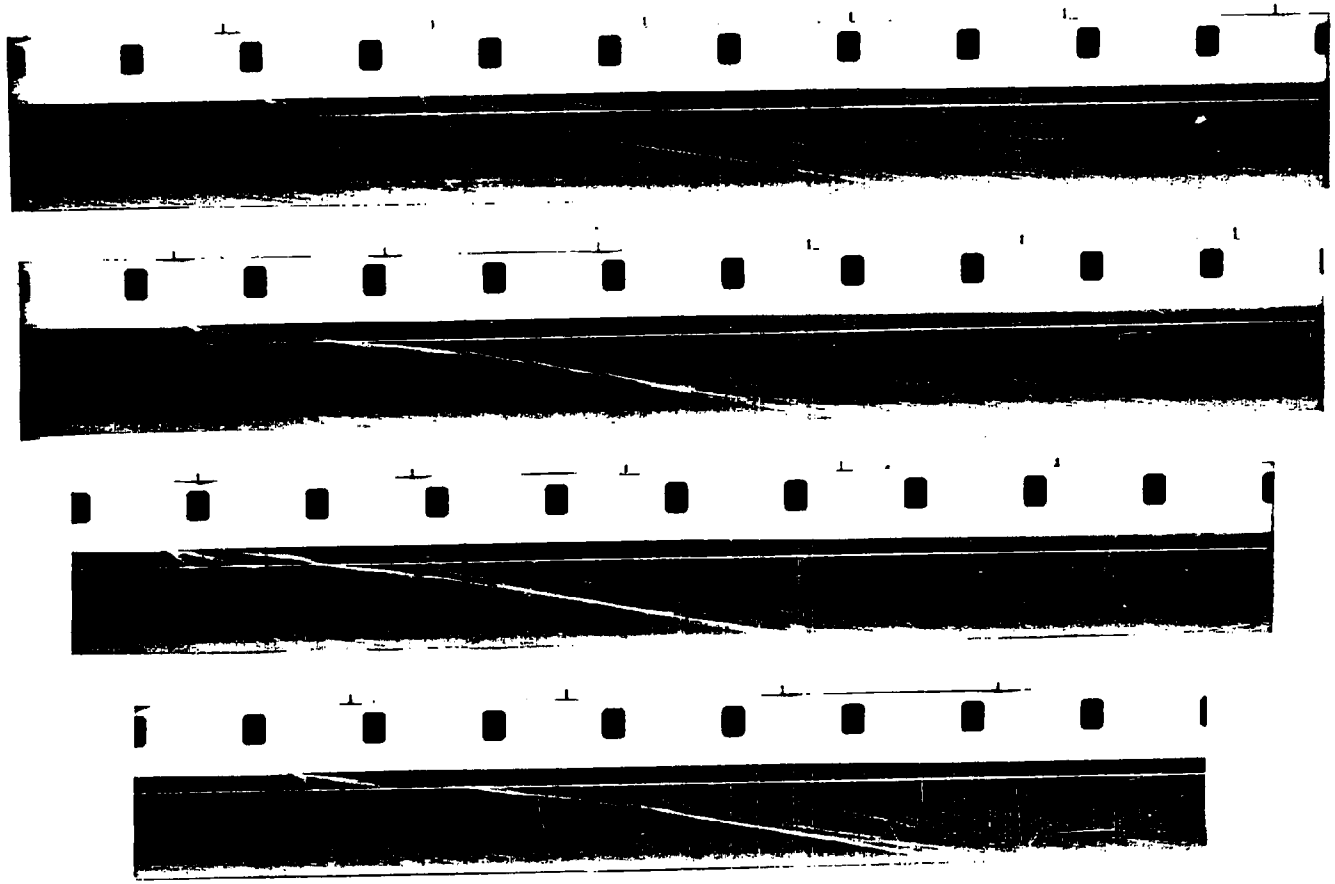

FIG.19 SCHLIEREN STREAK PHOTOGRAPHY FOR INTERMITTENT JET CREATED BY MECHANICAL "CONVERTER" WITH PARALLEL WALLS (TEST OF 12 APRIL 62)

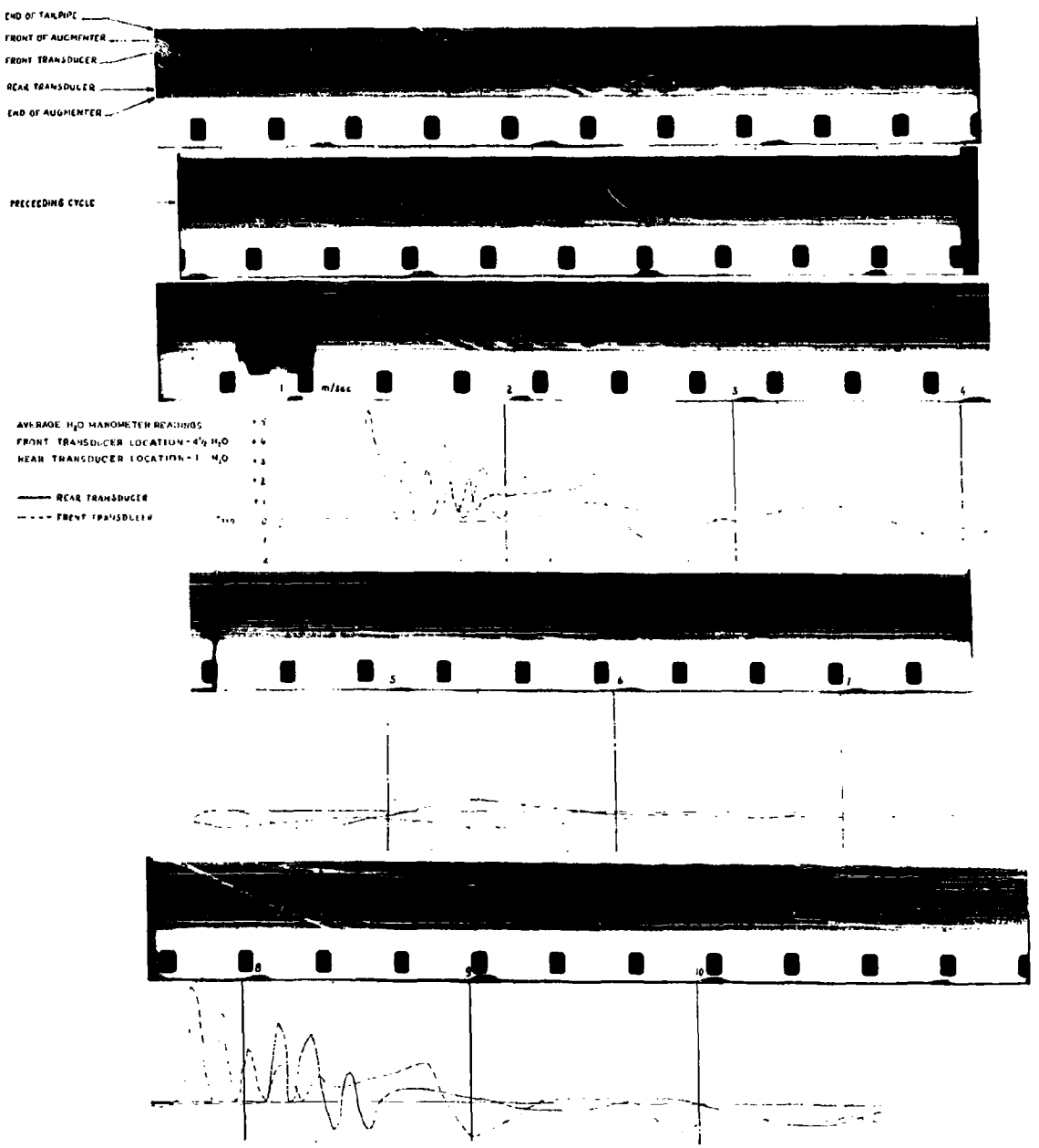

FIG. 20 SCHLIEREN STREAK PHOTOGRAPHY AND ASSOCIATED PRESSURE RECORD FOR INTERMITTENT JET CREATED BY MECHANICAL "CONVERTER" WITH 8" DIVERGENT AUGMENTER (TEST OF 20 JUNE 62, ROLL B)

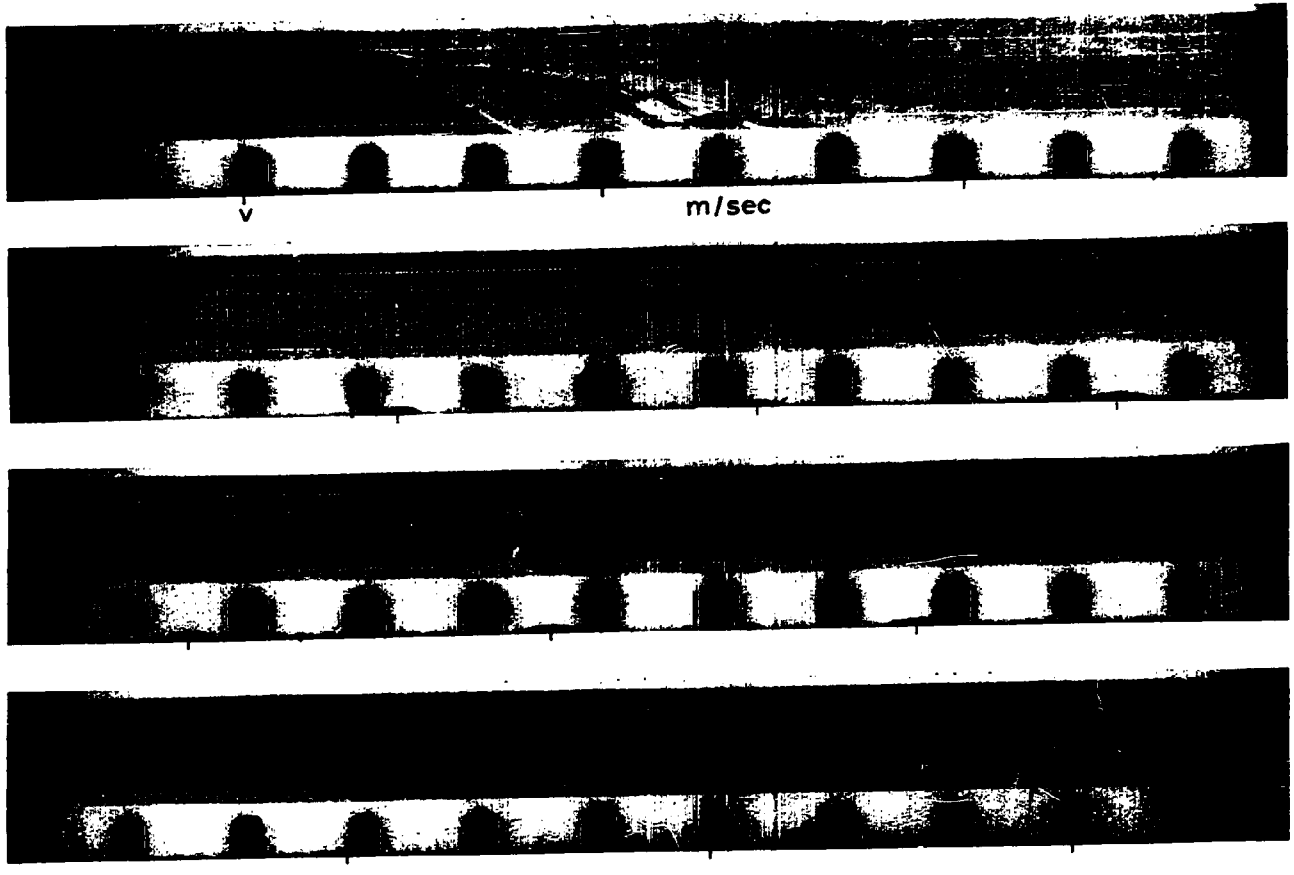

FIG. 21 JET CAUSED BY A SINGLE EXPLOSION IN THE PRIMARY JET TUBE
(TEST OF 11 JUNE, 62)

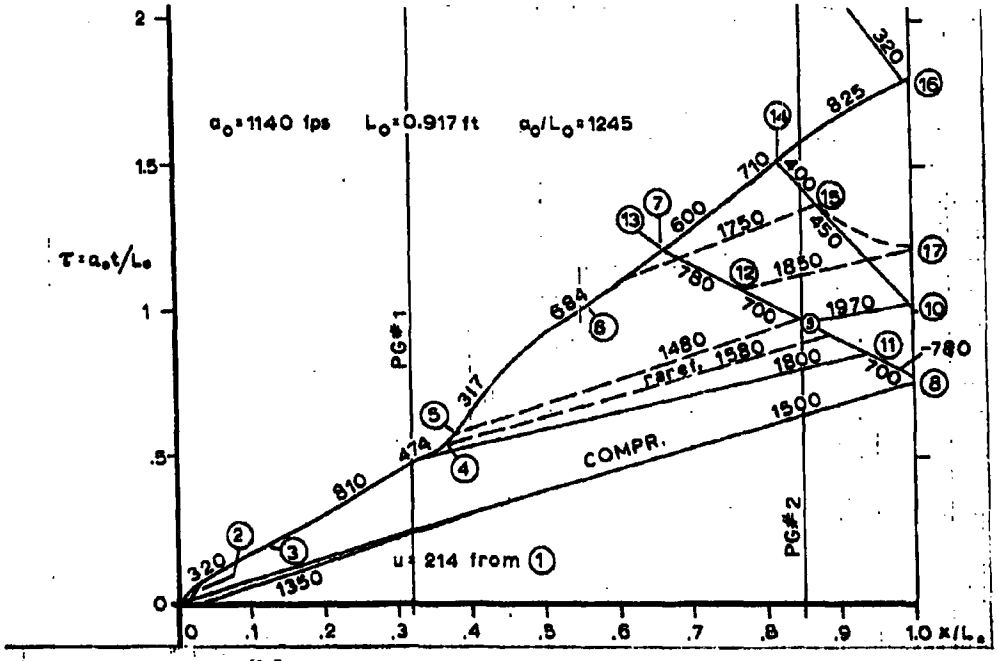

Point	Sta. x/L_o	$(\frac{a_o}{L_o})t$	Velocity U, fps	$U=\frac{u}{a_o}$	u+a fps	$\frac{u+a}{a_o}$	u-a	$\frac{u-a}{a_o}$	P	Q	$\frac{a}{a_o}=A_o$	$\frac{p}{p_o}=A_o^7$
1	0	-.323	214	.1875	1351	1.185			5.170	4.795	.9965	
2	0	0	317	.278	1350	1.335			5.56	5.000	1.057	1.475
3	.17	.262	810	.710	2110	1.850			6.40	5.000	1.14	2.5
4	.33	.474	474	.416	1910	1.677			5.836	5.000	1.083	1.75
5	.20	.500	317	.278	1520	1.385			5.56	5.000	1.057	1.475
6	.55	1.00	684	.600	1960	1.72			6.20	5.000	1.12	2.21
7	.70	1.25	600	.526	1860	1.63			6.046	5.000	1.105	2.08
8	1.00	.78	360	.316	1500	1.315	-780	-.684	5.316	4.684	1.00	1.00
9	.86	.95	360	.316	1500	1.315	-780	-.684	5.316	4.684	1.00	1.00
10	1.00	1.03	830	.728	1970	1.730	-310	-.272	5.726	4.272	1.00	1.00
11	.95	.85	550	.482	1800	1.58	-700	-.614	5.96	5.00	1.097	1.915
12	.77	1.1	575	.504	1850	1.62	-700	-.614	6.09	5.07	1.117	2.17
13	.67	1.2	600	.528	1790	1.57	-590	-.518	5.736	4.684	1.042	1.335
14	.82	1.5	710	.613	1810	1.59	-400	-.351	5.433	4.207	.965	.78
15	.875	1.38	650	.570	1750	1.535	-450	-.395	5.38	4.24	.962	.76
16	1.00	1.2	710	.622	1850	1.62	-430	-.377	5.62	4.38	1.000	1.00
17	1.00	1.8	823	.721	1960	1.721	-320	-.279	5.721	4.28	1.00	1.00

FIG. 21a: TIME-DISTANCE WAVE DIAGRAM AND TABULATED METHOD OF CHARACTERISTICS PARTIAL ANALYSIS OF SCHLIEREN RECORD OF FIGURE 21

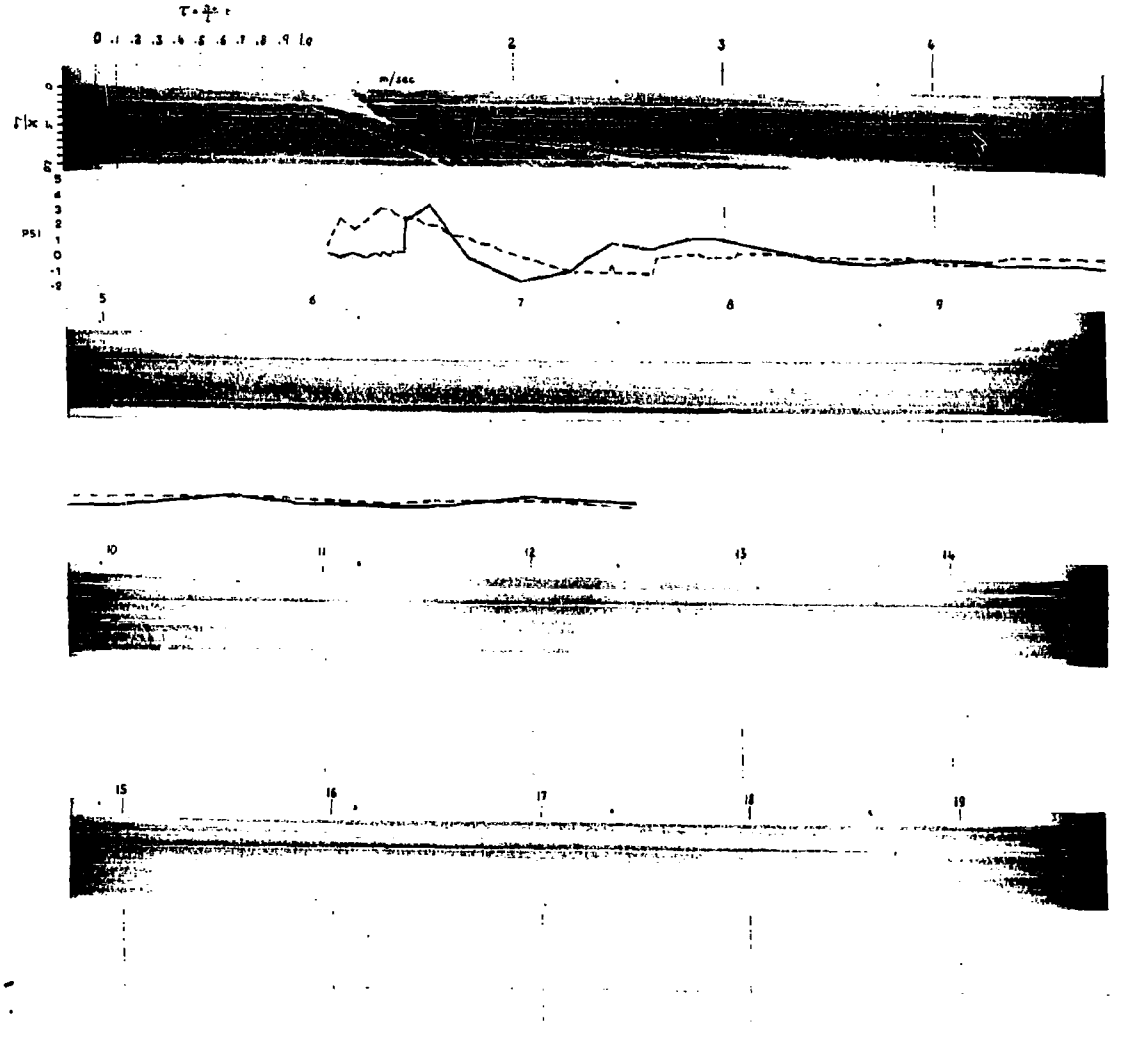

FIG. 22 JET CAUSED BY A SINGLE EXPLOSION IN THE PRIMARY JET TUBE
(TEST OF 20 JUNE 62, ROLL A)

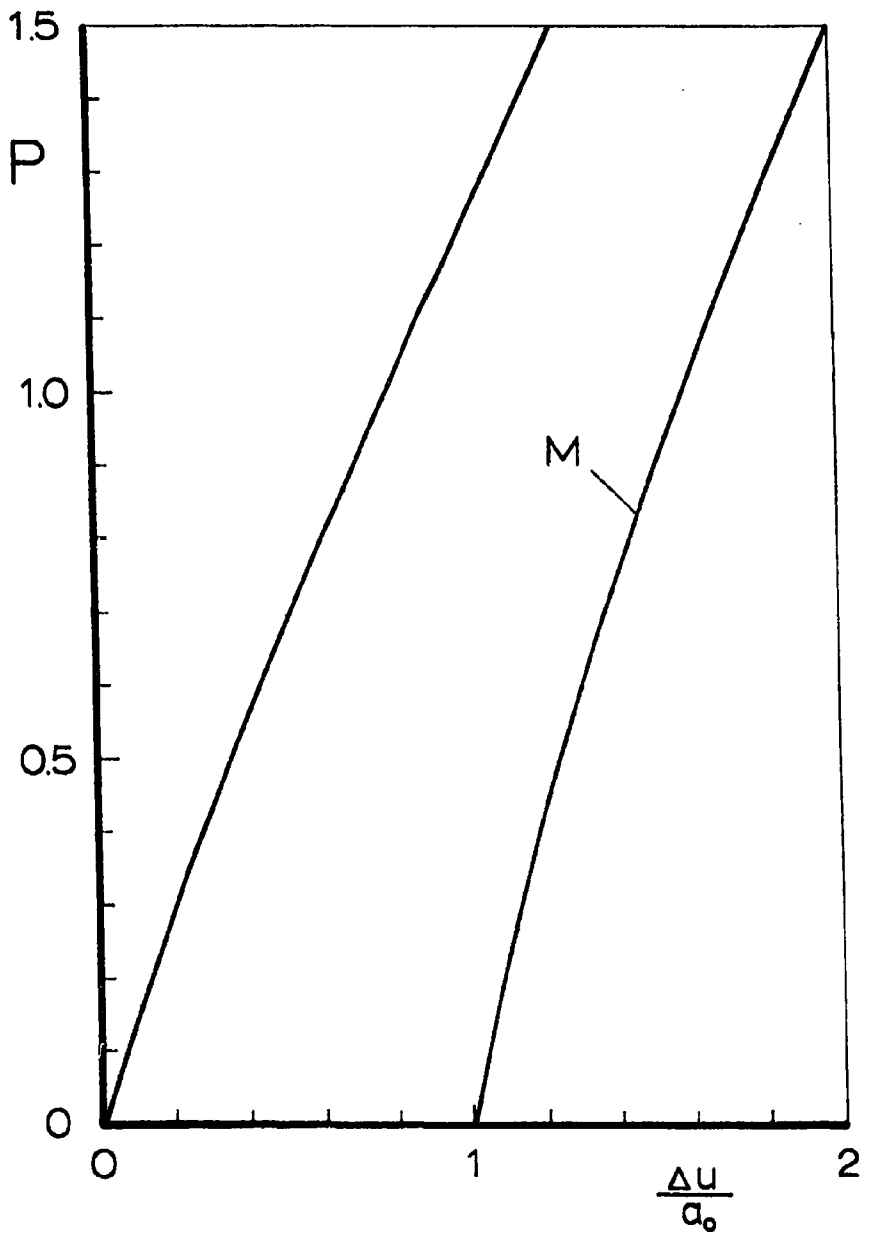

FIGURE 23: SHOCK POLAR where $P = \ln p/p_o$ and $\gamma = 1.4$

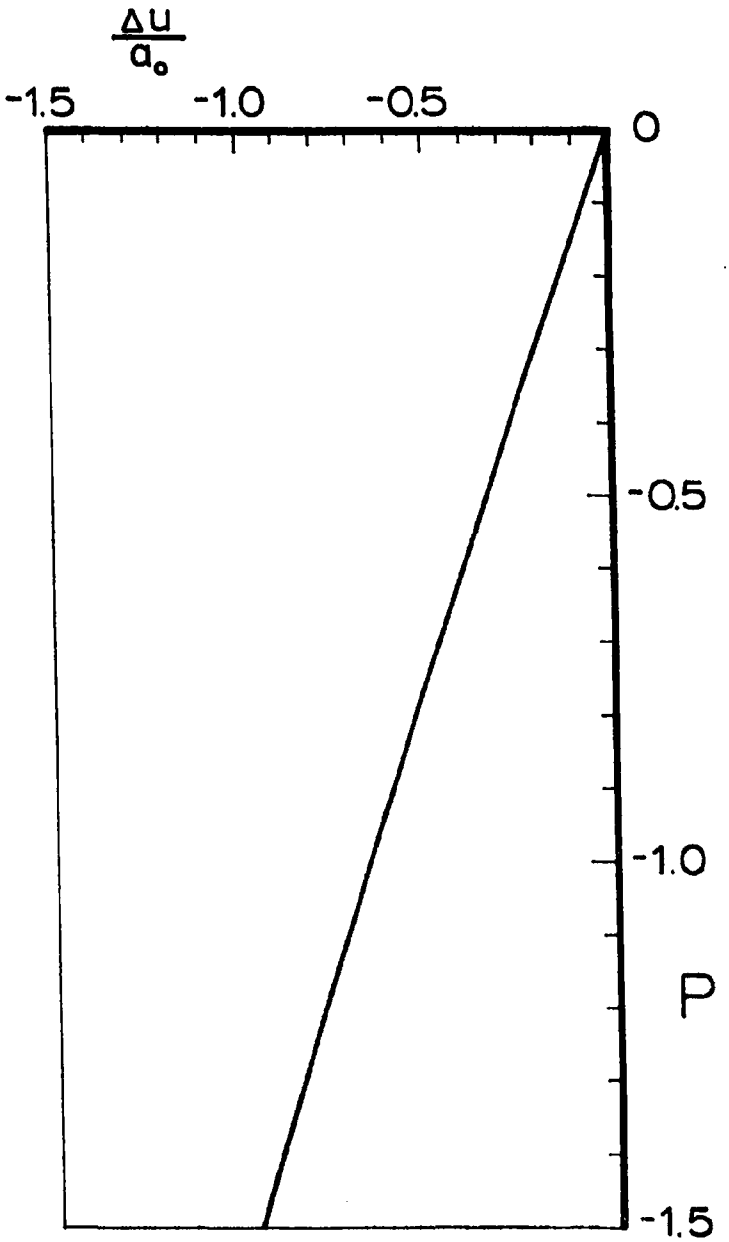

FIGURE 24: RAREFACTION POLAR where $P = \ln p/p_o$ and $\gamma = 1.4$

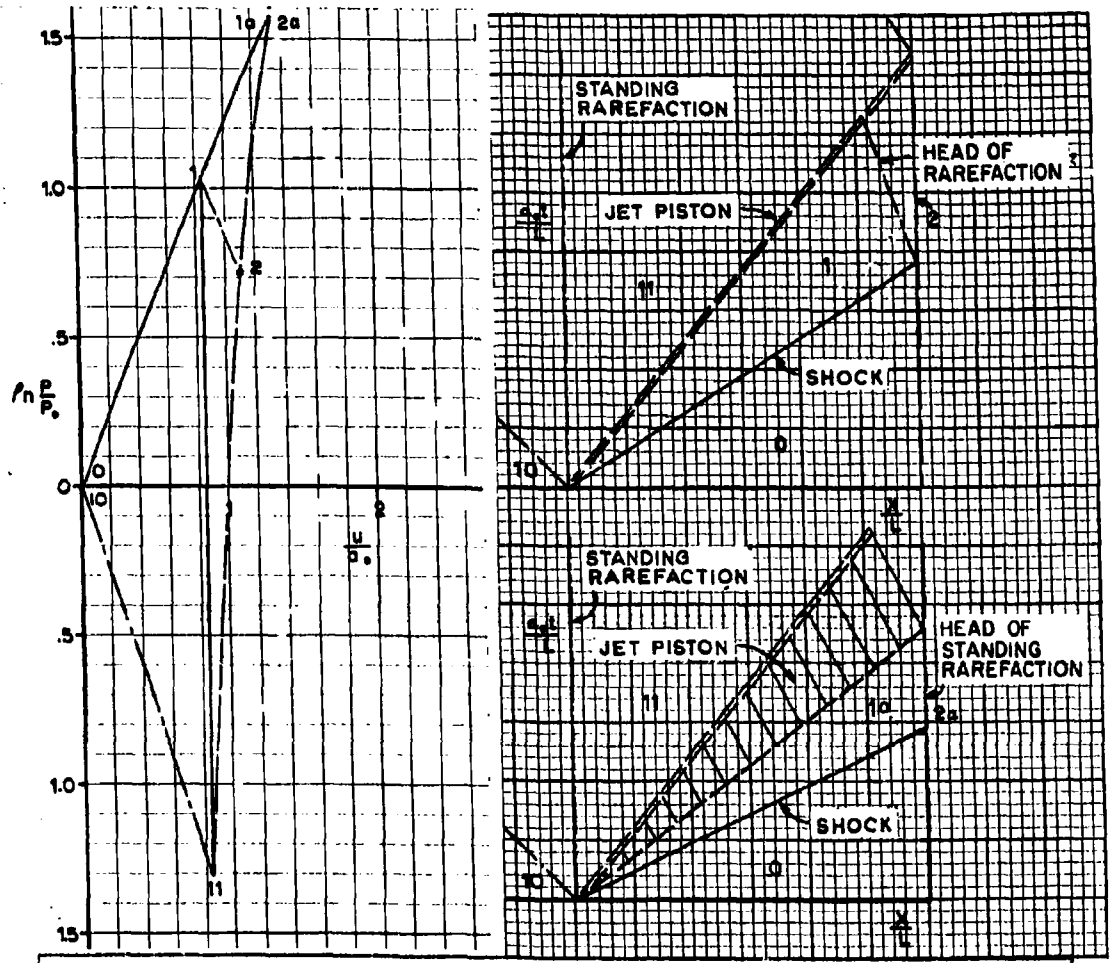

State	M	ln p/p_o	$\frac{p}{p_o}$	ln a/a	$A=a/a_o$	U	V	U+V	U+A	U-A
0	0	0	1	0	1	0	0	0	1.00	-1.00
1	1.62	1.04	2.90	.17	1.185	.84	1.62	1.62	2.025	- .345
10	0	0	1	0	1	0	0	0	1.00	-1.00
11	-1 -1	-1.305	.271	-0.186	.83	.83	-.83 -1	0 -1	+1.66	0
2	-1 -1	0	1	0	1	1.64	-1.185 -1	- .355 + .64	2.64	+ .64
1a	2.067	1.57	4.82	.277	1.32	1.32	2.067	2.067	2.64	0
2a	-1 -1	0	1	0	1	2.6	-1.32 -1.06	0 1.54	3.66	.54

FIGURE 25: VECTOR-POLAR AND TIME-DISTANCE DIAGRAMS FOR PASSAGE OF A THIN HIGH-VELOCITY PISTON THROUGH A THRUST AUGMENTER

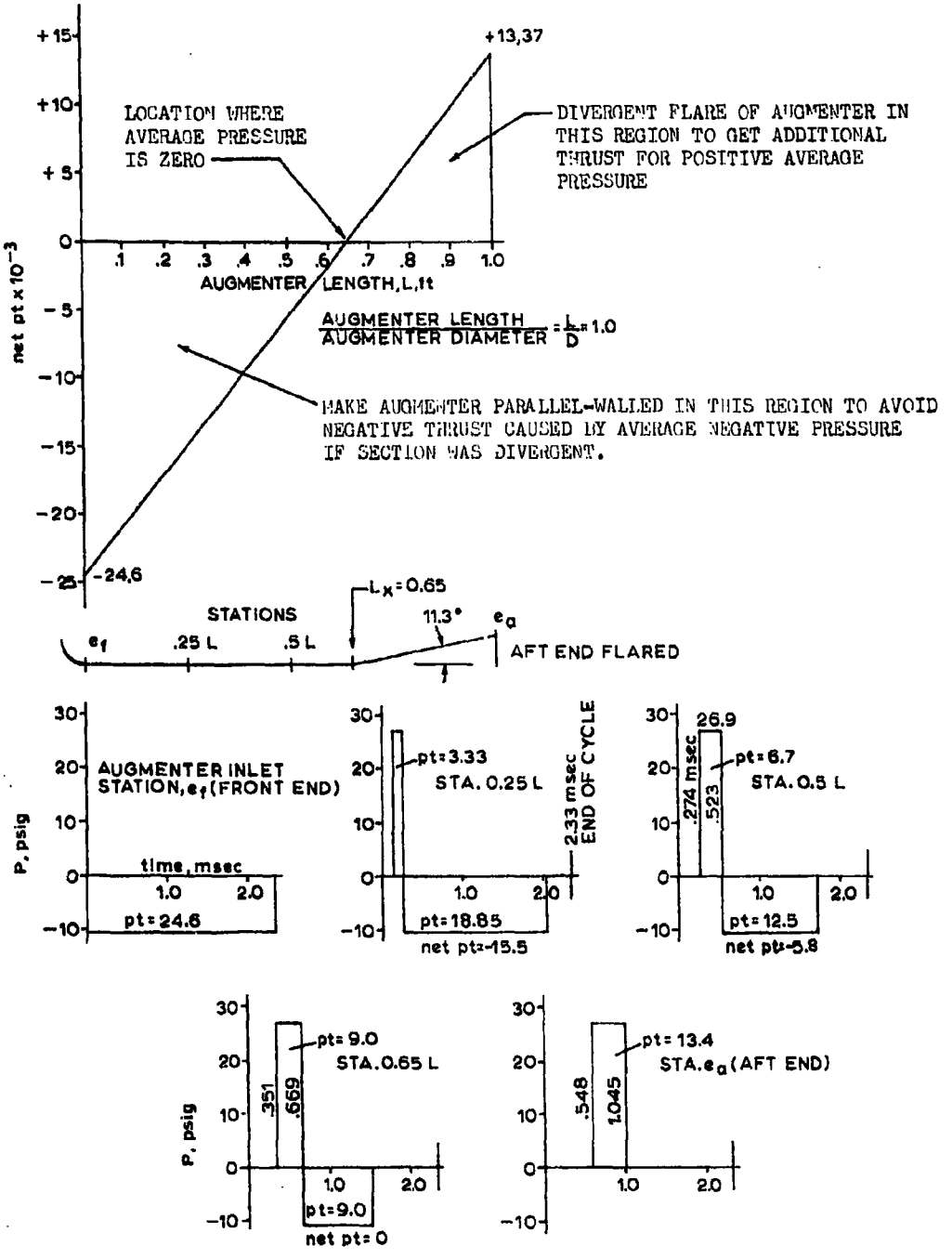

FIG. 25a: PRESSURE-TIME AND PRESSURE-IMPULSE LOCATION FOR PASSAGE OF A THIN HIGH-VELOCITY PISTON THROUGH A THRUST AUGMENTER